NIMS 21
Research Accomplishments

The Twenty-one Key Research Accomplishments for the First Mid-Term
(FY2001 to FY2005)

NIMS
Independent Administrative Institution
National Institute for Materials Science
http://www.nims.go.jp/eng/index.html

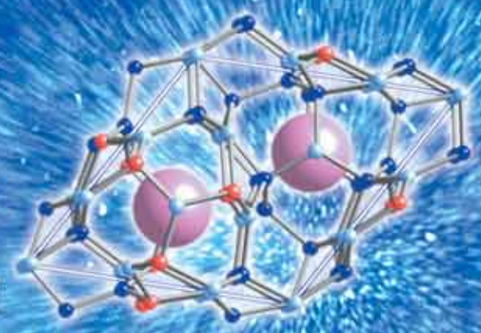

On Issuing "NIMS 21" Main Research Accomplishments during the First Mid-Term (FY2001-FY2005)

Teruo Kishi
President of NIMS

The National Institute for Materials Science (NIMS) was established on April 1, 2001 with the merger of two existing research institutions: the National Research Institute for Metals and the National Institute for Research in Inorganic Materials. The five years up to March 31, 2006 formed the first period of the Mid-Term Program as an independent administrative institution, and the second Mid-Term Program period started on April 1, 2006.

NIMS is a research institute that conducts fundamental research and basic investigation in the field of materials science. During the first Mid-Term Program, our priorities were to promote research on ‘nanomaterials’, ‘materials research for environment and energy’, ‘material research for safety’, and ‘research infrastructure/intellectual foundation’. We plan to select 21 major research accomplishments from the past five years and publish them in a booklet called ‘NIMS 21’ in order to introduce our research activities and achievements. We have also included sections describing relevant research fields to help develop a greater understanding of these fields.

During the first Mid-Term Program period, NIMS carried out many reforms and many new activities. We began operating the Nanotechnology Researchers’ Network Center of Japan, the International Center for Young Scientists, and the Doctoral Programs for the Graduate School at the University of Tsukuba.

The operation of the Nanotechnology Researchers’ Network Center was commissioned by the Ministry of Education, Culture, Sports, Science and Technology, and the center is helping to create networks for nanotechnology researchers through the sharing of research facilities and circulation of research information.

The International Center for Young Scientists attracts a wide range of young researchers of various nationalities and from diverse research fields, and gives them opportunities to conduct original research in new fields, in an inspiring environment that is international, interdisciplinary and cross-cultural.

The Doctoral Program in Materials Science and Engineering was established at the Graduate School of Pure and Applied Sciences at the University of Tsukuba as a joint graduate school major. It is a new type of joint graduate school and aims to foster high-level research professionals in the materials science and engineering fields. These activities closely relate to the operation concepts of NIMS, such as becoming an internationally open research institution, securing excellent human resources, and creating both an international and a domestic research network. We will continue these activities during the second Mid-Term Program period.

During the first Mid-Term Program period, the overall achievements of NIMS improved both quantitatively and qualitatively. Compared to the period before it became an independent administrative institution, the number of journal articles published increased by 1.9. Additionally, the number of citations in journal articles in the material science field of ISI increased by a remarkable 3.4 (1.8 times per article), and our world-ranking in this regard jumped astonishingly from 31st in the previous period to fifth in the post-independent administration period.

In terms of patents, both the number of applications and registrations have almost doubled, thus accelerating the transfer of technology to the private sector. Five venture companies have been created by making good use of the experiences developed by NIMS.

In addition, our operational activities have been re-energized. Internationally, we have signed The Memorandum of Understanding regarding collaborative global research with 73 institutions, exchanged agreements to establish sister institution relations with eight institutions, and have joint international graduate school programs with seven universities. The number of official visitors who annually pass through the Public Relations Office exceeds 2,000. We also actively participate in joint activities with industries, universities and independent administrative institutions, and promote approximately 300 collaborative research projects with institutions, such as private corporations and universities.

Further to the abovementioned efforts, as a COE in the materials science field, we have promoted activities under three main themes of: ‘strengthening international engagement’, ‘circulation of the knowledge base’ and ‘cooperation between independent administrative institutions, industry, and universities’. Specifically, measures include holding the World Materials Research Institute Forum (a forum in which representative institutions involved in leading international materials science research gather to exchange information regarding research trends and to create networks); publishing the Materials Science Outlook (white reports that summarize materials science research trends), and an international journal (Science and Technology of Advanced Materials); establishing the Materials Research Platform (an industry-focused forum where researchers from industries, universities and independent administrative institutions gather to circulate information and conduct collaborative research); and promoting international standardization and joint research between universities and independent administrative institutions. The basic outline of these measures was established during 2004, relevant activities began in 2005, and we are continuing to promote them strongly in the second Mid-Term Program period starting from 2006.

We believe that NIMS should focus on nanotechnology driven materials science for sustainability in the second period. Based on this concept, in the second Mid-Term Program period our priorities are to conduct 20 research projects with respect to the nanotechnology driven creation of new materials as well as material upgrading that responds to social needs.

It is the mission of NIMS and other public institutions to thoroughly promote fundamental research and basic investigation, which is necessary for long-term stabilization. NIMS will continue to be a research institution that actively explores something new and evolves continuously.

INDEX

1 Atomic Switch

■ EXECUTIVE SUMMARY

At present, the miniaturization of semiconductor transistors has reached its limit. To achieve sustainable development of an advanced information society, a device implementing new functions or principles different from those of miniaturization needs to be developed. The "atomic switch" is a nanodevice based on a new principle of operation that involves controlling the movement of atoms instead of electrons, and can be considered as a type of mechanical switch. Using this nanodevice, the elements of the nanoscale dimensions have made it possible to realize a function beyond that of the semiconductor transistor.

■ OUTLINE

An atomic switch is composed of an electronic and ionic mixed conductor (hereafter, mixed conductor), electrode, and metal electrode, which are placed approximately 1 nm apart (Fig. 1). When the proper voltage is applied between these two electrodes, an electrochemical reaction occurs, with which the formation and disappearance of a cross-link of metal atoms between the electrodes can be controlled. More specifically, when a positive voltage is applied to the mixed conductor electrode, metal ions in the mixed conductor electrode are reduced by tunneling electrons emitted from the metal electrode and then deposited on the electrode surface.

A cross-link is formed between the electrodes by these deposited metal atoms, which means "the switch is turned on". When a negative voltage is applied, the deposited metal atoms are ionized and return to the mixed conductor electrode. As a result, the metal atom cross-link disappears, which means "the switch is turned off".

In a semiconductor transistor, the density of electrons in the semiconductor is controlled using a gate electrode. In contrast, in the atomic switch, the formation and disappearance of the metal atom cross-link, which acts as a path for electrons, are controlled, and hence, the element structure is geometrically changed. Therefore, the atomic switch can be considered as a mechanical switch. A mechanical switch is usually considered to have a low operating speed. However, the atomic switch can perform at speeds as high as that of semiconductor devices because the metal atoms need to move only a short distance of approximately 1 nm. In addition, even if the dimensions of the elements are on the nanoscale, the atomic switch can maintain a very low "on resistance" because its "on state" is realized by metal atoms. Figure 2 shows the relationship between the element dimensions and on resistance of a semiconductor transistor. Although an increase in the on resistance, which is directly related to an increase in electric power consumption, is a serious problem, it does not occur in the atomic switch. Furthermore, the atomic switch is a nonvolatile device because the metal atom cross-link formed remains in a steady state even when the applied voltage is removed.

The atomic switch has a simple structure and can be produced within approximately one-fourth of the process (cost) of the semiconductor transistor. Figure 3 shows an electron microscope image of a prototype of the atomic switch

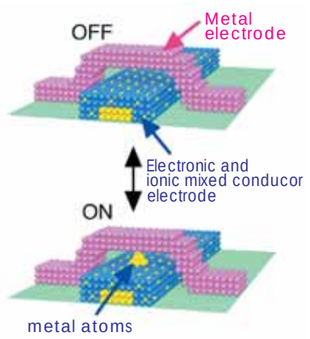

Fig.1 Schematic of atomic switch.

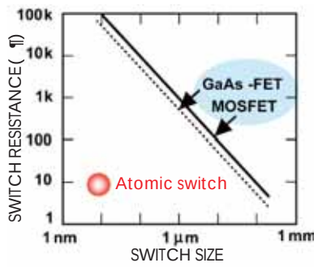

Fig.2 Relationship between element dimensions and resistance.

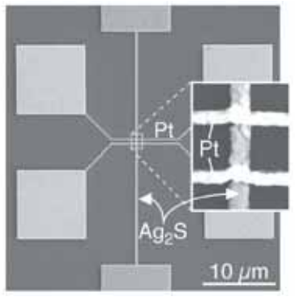

Fig.3 Electron micrograph of atomic switch.

fabricated using silver sulfide (Ag_2S) as the mixed conductor and platinum (Pt) as the metal. The atomic switch shown in Figure 1 is formed at the intersection of a silver sulfide wire and a platinum wire. Because this switch can be fabricated by conventional microfabrication processes, the atomic switch can be easily mounted on present semiconductor devices. Therefore, the atomic switch can be considered one of the devices most applicable for practical use.

■ ACHIEVEMENTS

Using developed integration technology, we fabricated basic logic circuits, namely, AND, OR and NOT circuits, and confirmed their operations.[1] According to information processing theory, any logic circuit can be constructed by simply combining these three basic logic circuits. Therefore, it is inferred that any computer circuit can be constructed with only atomic switches. Furthermore, the atomic switch has excellent features, such as nonvolatility, low on resistance and learning capacity, in addition to its small size. The use of these outstanding features enables the development of an electronic device that cannot be realized with only semiconductor transistors. For example, when the atomic switch is applied to a switching circuit of a programmable logic device, a size of one-thirtieth and an on resistance of one-fortieth or less that of the conventional switching circuit can be achieved. As a result, the number of switches and logic operation blocks that can be mounted on the circuit is one or more orders greater than that for the conventional circuit. Therefore, a next-generation programmable logic device that is capable of performing any function with one chip will become feasible. Thus far, we have succeeded in fabricating a prototype basic switching circuit and demonstrating its performance jointly with a private company.[2] We are now furthering our research and development, aiming for early commercialization.

PUBLISHED RESEARCH PAPERS

1) K. Terabe, T. Hasegawa, T. Nakayama and M. Aono: *Nature* 433 (2005) 47.

2) S. Kaeriyama, T. Sakamoto, H. Sunamura, M. Mizuno, H. Kawaura, T. Hasegawa, K. Terabe, T. Nakayama and M. Aono: *IEEE J. Solid-State Circuits* 40(1) (2005) 168.

ADDITIONAL INFORMATION ABOUT ELECTRONIC AND IONIC MIXED CONDUCTORS

When an electric field is applied to a metal or semiconductor, electrons move to induce a current flow. Alternately, in an ionic conductor, ion movement causes a current flow. An ionic conductor in which ions are the main current carriers is called a solid electrolyte (pure ionic conductor), and an ionic conductor in which not only ions but also electrons behave as current carriers is called an electronic and ionic mixed conductor. The silver sulfide used for the atomic switch is an example of an electronic and ionic mixed conductor. Silver sulfide is an ionic crystal, in which positive silver ions (Ag^+) and negative sulfur ions (S^-) exist (Fig. 4). When an electric field is applied to this crystal, Ag+ ions will move to the negative electrode through a lattice composed of S- ions as if flowing through a liquid. The ionic conductor has also been used as the material for solid-state batteries, and is one of the materials applicable to both traditional and new technologies. In the study of the atomic switch, we can realize a device that functions as a mechanical switch, using the excellent features of the electronic and ionic mixed conductor and nanotechnology.

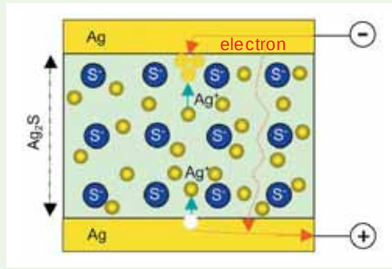

Fig.4 Electronic and ionic mixed conductor.

INQUIRIES
Nano System Functionality Center Tsuyoshi Hasegawa
E-mail :HASEGAWA.Tsuyoshi@nims.go.jp

2 Development of the Nanotester

■ EXECUTIVE SUMMARY

We are using nanotechnology, which is a key technology in the twenty-first century, to develop new "nanoelectronics," with the aim of markedly improving the performance of computers. We need to clarify how easily current flows in an ultra small electrical component of size close to the nanometer scale, which is related to electrical resistance. However, there have not yet been any methods to measure the resistance of such nanoscale components. We developed a new device, the "nanotester," which enables the measurement of such electrical resistance.

■ OUTLINE

Nanoelectronics is a new field of electronics, in which circuits are constructed using ultra small components of size close to the nanometer scale. When designing and establishing such ultra fine circuits, it is essential to know the electrical resistance of each component. Nevertheless, there have been no general methods for measuring the resistance of nanoscale electrical components.

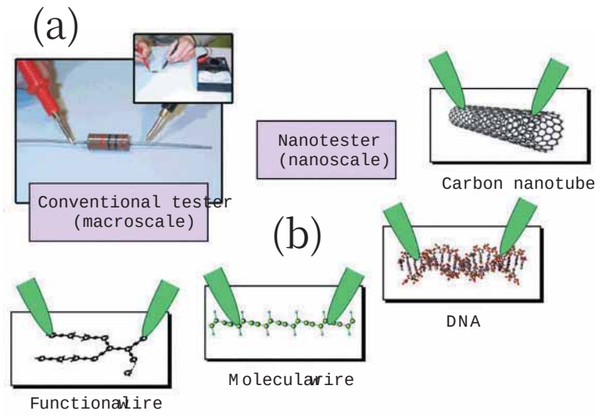

Fig. 1 (a) Conventional tester. (b) Nanotester developed.

The tester for measuring the electrical resistance of a conventional macroscale electrical component is well known (Fig. 1(a)). We now need a similar measurement tool for nanoscale electrical components (four examples of which are shown in Fig. 1(b)). However, the size of the nanoscale component (~10 nm) is one-millionth that of the macroscale component (~10 mm). Therefore, it is essential to reduce the diameter of the electrode bar of the tester one-millionfold from approximately 1 mm to 1 nm. To accomplish this, we developed an innovative scanning tunneling microscope (STM), in which a quantum "tunneling current" flows between a sharp metal needle (the tip diameter of which is in the atomic scale to nanometer scale range) and the sample. Using this STM, we can observe and identify each atom on the sample surface. We propose to use 2, 3 or 4 metal probes for the STM. Each probe can be operated independently and enables high-resolution imaging such that individual atoms can be identified. Furthermore, the critical feature of the multiprobe device is that each probe comes into contact with the sample surface exactly at the point determined from the observed image to carry out the electrical measurement as a "nanotester."

For most research, "saying is one thing, doing another." There have been many hurdles to overcome in the past several years. This nanotester has finally attained the level of practical use in the last few years. Owing to the promotion of the research project supported by the Ministry of Education, Culture, Sports, Science and Technology, a method of controlling the multiprobe tester by computer has also been developed. In the following section, we describe an example of measurement by this method.

■ ACHIEVEMENTS

We succeeded in measuring the electrical resistances of various nanoscale structures, including carbon nanotube, fullerene (C_{60}), a conductive polymer thin film and a metal nanowire, using the developed nanotester.

Fig.2 shows an example. Fig.2(a) shows an STM image of a metal nanowire ($ErSi_2$ nanowire formed on a silicon surface) observed using one of the two nanotester probes. The thickness and height of the metal nanowire were found to be 3 nm and 1 nm, respectively. The two probes with ultra sharp tips (refer to "Additional Information about Measurement of Nanoscale Devices" below) were brought into contact with this nanowire, as shown in the inset of Fig. 2(b), and the electrical resistance between the probes was measured. Fig. 2(b) shows the results of this measurement, obtained by varying the distance between the probes. According to the slope of the straight line fitted to the measured values, the electrical conductivity of this metal nanowire is 1.9 kΩ・nm^{-1}. This is the first time that the electrical conductivity of a nanowire has been measured.

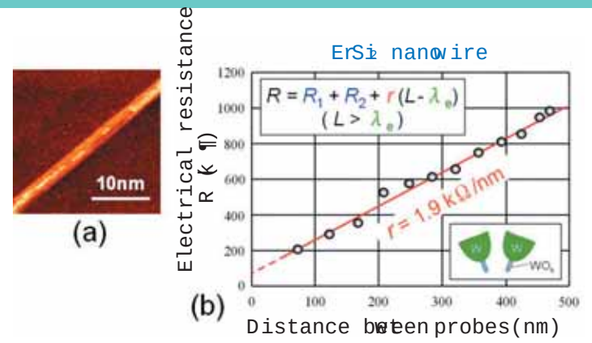

Fig. 2 (a) Metal nanowire ($ErSi_2$ nanowire formed on silicon surface). (b) Result of measuring electrical resistance of nanowire shown in (a).

PUBLISHED RESEARCH PAPERS

1) "Electrical Conductivity of Low-Dimensional Nanostructure", M. Aono, T. Nakayama, Y. Kuwabara and M. Akai: *Appl. Phys.* 75 (2006) 285.

ADDITIONAL INFORMATION ABOUT MEASUREMENT OF NANOSCALE DEVICES

To measure the electrical resistance of the smallest possible components, the probe of the nanotester should be as fine as possible . This is comparable to a situation in which tweezers are required to pick up a sesame seed, or two fingers are used to pick up a bean, which is much larger. The sharpness, namely, the curvature radius, of a probe tip made of a common metal, such as tungsten, is at least a few ten nm. We developed a method to form a rod of low-oxide tungsten WOx (good conductor) with a diameter of a few nm at the probe tip. Using this probe with the rod, we directly measured the electrical resistance of a metal nanowire for the first time ever.

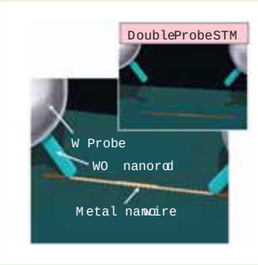

Fig. 3 An ultra sharp probe (for example, WOx nanorod) is required for the nanotester.

INQUIRIES
Nanosystem Functionality Center Tomonobu Nakayama
E-mail: NAKAYAMA.Tomonobu@nims.go.jp

3 Deep UV LED of Semiconducting Diamonds

■ EXECUTIVE SUMMARY

Semiconducting property of diamonds contributes to electronic devices. With the development of diamond pn junction, a UV light emission of 235 nm was detected for the first time in diamond light emitting diodes (LED). This success is a result of a technique used to produce an n-type semiconducting diamond established in 1997. The pn junction diode was found to be appropriate for photo diodes of deep UV light.

■ OUTLINE

A variety of materials, such as Si, Ge, GaAs, etc. are known to be semiconductors. Diamond is also semiconductors. Diamond is unique because their band gap is as high as 5.5 eV, which is much bigger than that of the well-known blue GaN (3.0 eV) LED. Diamonds, therefore, have the potential to emit UV light, the wavelength of which is shorter than that of GaN LED.

A high-level growth technique is required to make high quality diamonds that contain controlled amounts of doped impurities and low-density defects.

Fig. 1 shows a microwave assisted chemical vapor deposition apparatus in which semiconducting diamonds are grown. A mixture of gases, methane (CH_4) and hydrogen (H_2), is introduced into the apparatus chamber, and the gas decomposes in plasma to form diamond film on the substrate in the chamber.

When a single crystal diamond is used as the substrate, a high quality diamond film is readily deposited. In this process, boron or phosphorus is added to the CH_4 - H_2 system, and it is doped in the grown diamond. p-Type and n-type diamonds are made by doping boron and phosphorus, respectively. Fig. 2 shows a diamond specimen on which p- and n-type diamond films have formed. The specimen is black due to the presence of boron in the diamond substrate. Metal electrodes are dots from which gold wires extend to an electric source.

Blue light emission, as shown in Fig. 3, is observed from the pn-junction when an electric current is supplied from the source. UV light of 235nm is emitted, although blue emission is also visible, in the picture.

Fig. 1 Apparatus for CVD diamond synthesis.

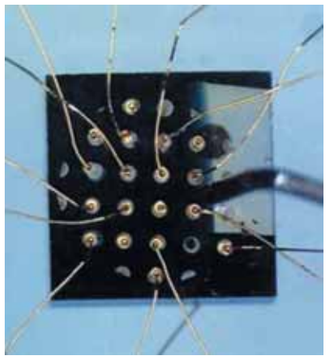

Fig. 2 Diamond substrate on which diamond pn junction film is formed.

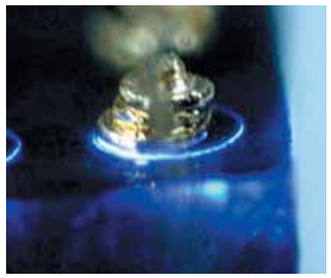

Fig. 3 Light emission from diamond pn junction.

■ ACHIEVEMENTS

Success in CVD diamond synthesis by the former NIRIM, in 1981, triggered active worldwide research from the 1990s. Another breakthrough in NIRIM diamond research was the synthesis of the n-type semiconducting diamond, developed in 1997[1].

It was inevitable that electronic applications established both p- and n- type diamond synthesis technology. It had previously been impossible to make n-type, while p-type diamonds were regularly developed. The NIRIM group succeeded in producing the n-type diamond with doping phosphorus. Following this success, pn junction was fabricated by the sequential deposition of p- and n- type diamond films, and for the first time, it was found that the junction has a rectification character and emits UV light as shown in Fig. 3[2]. It was also found that the pn-junction serves as a UV light detector.

Recently, the n-type property has been improved dramatically and the electron mobility of n-type diamonds has reached a world record 660 cm^2/Vs[3].

PUBLISHED RESEARCH PAPERS

1) S.Koizumi, M.Kamo, Y.Sato, H.Ozaki, T.Inuzuka, *Appl.Phys.Lett.* 71 (1997) 1065-1067.

2) S. Koizumi, K.Watanabe, M. Hasegawa and H. Kanda, *Science* 292 (2001), 1899-1901

3) M.Katagiri, J.Isoya, S.Koizumi, H.Kanda, *Appl. Phys. Lett.* 85 (2004) 6365-6367

ADDITIONAL INFORMATION ABOUT DIAMONDS

Diamond gem

Diamond cutting tool

Electronic devices
of which diamond has potential

In addition to being used for jewelry (as shown above), diamonds have the potential to be applied to various fields. As diamonds are the hardest material, mechanical diamond-cutting tools have been developed for the manufacturing industry. Electronic devices, such as high power transistors and light emitting diodes, are other applications for which diamonds have potential, due to their wide band gap semiconductor properties.

Diamonds can be made in two different ways: the high-pressure method, where graphite or charcoal is transformed into diamond under conditions of 5 GPa ultra high-pressure, and the chemical vapor deposition (CVD) method, where gases, such as methane, decompose into diamond.

INQUIRIES

Sensing Materials Center Hisao Kanda
E-mail: KANDA.Hisao@nims.go.jp

4 Development of Simulation Method for the Evolution of the Nanostructure in Real Materials

■ EXECUTIVE SUMMARY

Nanoscale microstructure control is the key technology for developing advanced materials with excellent properties because the materials properties, such as mechanical, magnetic, and electric properties, crucially depend on its microstructure morphology. In this study, we established the first step in the development of the computational materials design system based on phase-field simulation [1-4].

■ OUTLINE

Recently, the phase-field method [1-4] has been developed in many fields of materials science as a powerful tool to simulate and predict complex microstructure development. The phase-field method is a computational method in which the microstructural morphology of materials is expressed based on a continuum model, and the temporal/spatial changes in complex microstructures are analyzed using evolution equations. The objects of simulation by this technique now extend to the field of materials science as a whole, and its use is continuing to grow as a complete microstructural evolution analysis/simulation method. In our current research, we developed a simulation method for the microstructural evolution of practical real materials based on the phase-field method. Since the complex microstructure changes can be modeled quantitatively by using the frame of the phase-field method, it is expected to become a strong tool in materials design.

■ ACHIEVEMENTS

The following figures are typical examples of phase-field simulation for microstructure developments in various types of structural and functional materials. The complex morphological microstructure evolution in real materials is simulated reasonably.

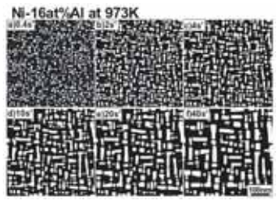

Coarsening behavior of γ' precipitates (white particles) in a Ni-base superalloy. The shape of the precipitates become square due to an elastic constraint, and the particles align in the <100> direction.

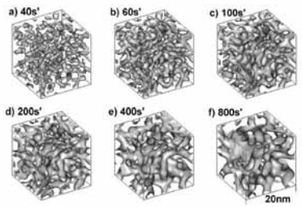

3D simulation of the spinodal decomposition in Fe-Cr stainless alloy. An isotropic mottled structure is formed.

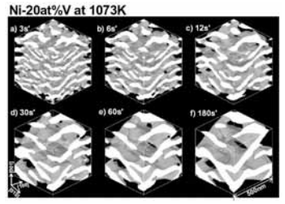

3D simulation of the coarsening of γ'' phase in Ni-V alloy. The slanted lamellae microstructure is formed by the elastic constraint.

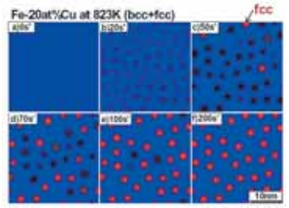

Phase separation of the _ phase (bcc) in Fe-Cu alloy, and the structural transformation of α-Cu (bcc) to the γ phase (fcc). Black particles are α-Cu (bcc) , and red parts correspond with the fcc structure.

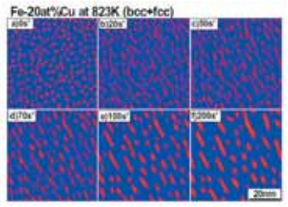

Shape change of γCu phase during coarsening. The rod shaped precipitates develop with aging

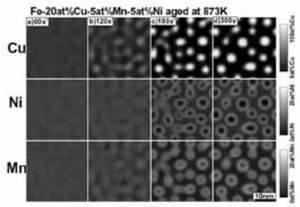

Phase decomposition process of the α phase (bcc) in the Fe-Cu-Mn-Ni quaternary system. The Mn and Ni components initially concentrate in the Cu precipitation phase, but segregate to the interface as the Cu concentration in the particles increases.

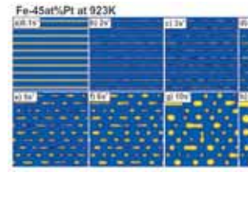

The spheroidization process in a lamellar microstructure. The lamellar structure in its initial state breaks down, and spheroidization occurs during diffusion controlled microstructure evolution.

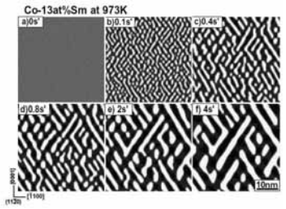

Phase decomposition process in Sm-Co-Cu alloy (white: Sm(Co,Cu)5, black: Sm2(Co,Cu)17). A modulated microstructure evolves from the mechanism of spinodal decomposition.

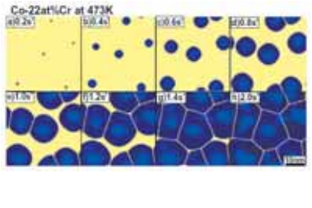

The microstructure evolution in Co-Cr magnetic thin film during sputtering. The blue part indicates the alloy phase, and the yellow part is a substrate. The Cr-rich phase appears at the grain boundary region in the phase decomposition within the alloy phase.

Combining the above-mentioned micro/nanostructure simulation with the image based materials property calculation is the next challenging issue to achieve a practical materials design and optimizing system that promptly searches for useful materials expressing the desirable properties.

PUBLISHED RESEARCH PAPERS

1) T.Koyama and H.Onodera, *J. Phase Equilibria and Diffusion,* 27(2006), 22.
2) T.Koyama and H.Onodera, *Mater.Trans.,* 46(2005), 1187.
3) T.Koyama and H.Onodera, *Mater.Trans.,* 44(2003), 1523.
4) T.Koyama and H.Onodera, *Mater.Trans.,* 44(2003), 2503.

ADDITIONAL INFORMATION ABOUT MICROSTRUCTURE CONTROL BY SOLID-STATE PRECIPITATION

「Nanostructure is controlled by solid-state precipitation」

Cooling hot brine produces salt crystal, as illustrated by the figure (left). This phenomenon, i.e. the appearance of the solute element from the solution, is called "precipitation". On the other hand, solid solution is the solution state of solid materials, and it is called "supersaturated solid solution" if the solute element is solved beyond its saturation limit. The solid-state precipitation is the precipitation process from the supersaturated solid solution (see right figure). Both the liquid state precipitation and the solid-state precipitation occur due to atom diffusion in the substance. In particular, since the diffusion rate is a lot slower in solid than in liquid, the diffusion distance of the solute element during the solid-state precipitation is a lot less than that in the liquid state. Therefore, the characteristic length of the microstructure formed by the solid-state precipitation is very small and it often provides nanoscale precipitates. As a consequence, nanostructure control becomes possible by applying the precipitation phenomenon to solids.

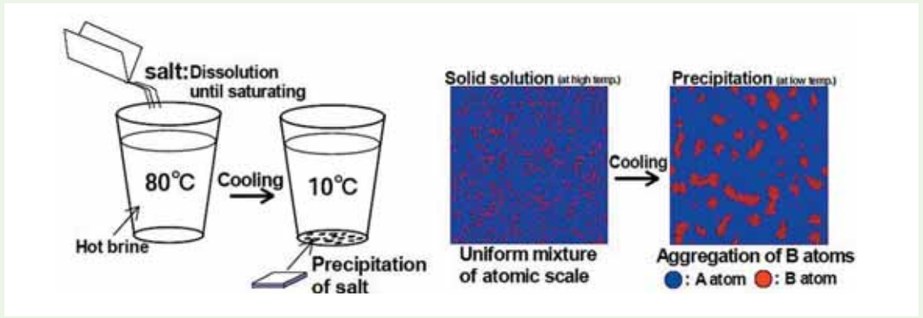

INQUIRIES
Computational Materials Science Center Toshiyuki Koyama, Hidehiro Onodera and Takahisa Ohno
E-mail: KOYAMA.Toshiyuki@nims.go.jp

5 Nanothermometer Using a Nanotube

■ EXECUTIVE SUMMARY

A nanothermometer is based on an accidental discovery made during a failure in GaN nanotube research. It was found that the phenomenon of expansion and contraction occurs reversibly in liquid gallium contained in carbon nanotubes in proportion to the change in temperature. Gallium in the tube was in a liquid state over a wide temperature range from a high of approximately 500℃ to a low of -80℃. A nanothermometer was successfully created using oxide nanotubes, such as MgO and SiO_2, which are more heat-resistant than carbon nanotubes. A carbon nanotube nanothermometer is recorded in the Guinness Book of World Records as the world's smallest thermometer.

■ OUTLINE

The nanothermometer discovery was accidental and serendipitous. This research started as a result of the failure in an attempt to synthesize a nanotube of gallium nitride (GaN) ahead of the world. Reacting carbon and gallium oxide in nitrogen at high temperature failed to generate a GaN nanotube, but instead produced a carbon nanotube containing metallic gallium. While observing the carbon nanotube under an electron microscope, we discovered by chance that the liquid gallium column contained in the tube expanded and contracted due to the heating effect of the electron beam. This is the same principle as the liquid mercury in a mercury thermometer, which expands with the external temperature. We found that it was possible to measure the sample temperature directly by accurately heating the sample under an electron microscope and measuring the change in the gallium column (heating it to approximately 500℃ above room temperature) (Fig. 1). We called the carbon nanotube showing the temperature reaction a "carbon nanothermometer", and it was recorded (in 2002) as the world's smallest thermometer in the Guinness Book of World Records (2004). To make the nanothermometer practical, it was necessary to develop a method to record the maximum temperature. We succeeded in developing a recording method by creating a gallium oxide membrane with an extremely small amount of oxygen. We also discovered a supercooling phenomenon whereby liquid gallium in the nanotube causes a volumetric change at a temperature of -80℃. This means that the nanothermometer can be used not only at high temperatures, but also at low temperatures (Fig. 2).

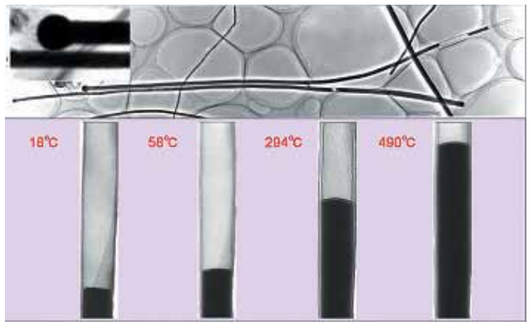

Fig. 1 Carbon nanotubes containing metallic gallium (upper diagram) Increase/decrease of liquid gallium columns in carbon nanotubes due to temperature changes under the electron microscope (lower diagram)

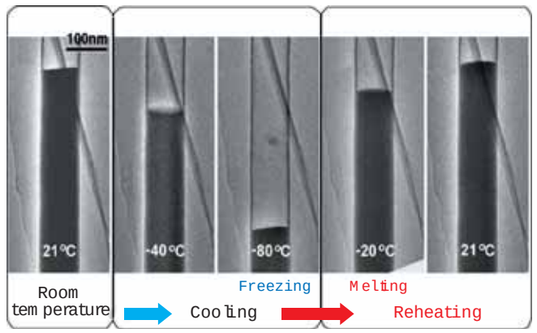

Fig. 2 Temperature reaction of a nanothermometer at low temperature Liquid gallium contained in carbon nanotubes freezes at -80°C and, when reheated, melts at -20°C.

Since a carbon nanotube is oxidized in air at approximately 500℃, it is necessary to create a nanotube with good quality thermal resistance and oxidation resistance to make a nanothermometer for practical use. For this purpose, we created oxide nanotubes of MgO and SiO_2 and developed a nanothermometer using such nanotubes (Fig. 3). A nanothermometer can be used as a temperature sensor to measure temperature in spaces at the micron level.

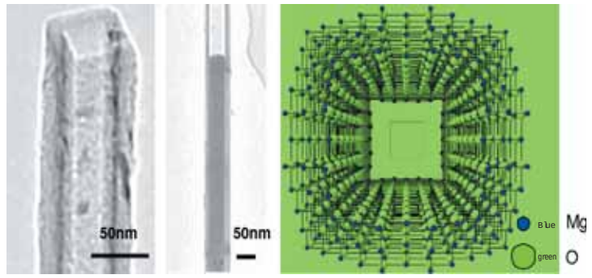

Fig. 3 Shape of single crystalline MgO nanotube (left), liquid gallium contained in the tube (middle), and structural model of an MgO nanotube (right)

■ ACHIEVEMENTS

(1) We discovered that a carbon nanotube containing liquid gallium can measure a temperature reaction, and it can be used as a thermometer in a wide range of temperatures from approximately 500℃ to -80℃.
(2) We proved that liquid gallium contained in the tube shows bulk characteristics (such as expansion coefficient).
(3) We developed a nanothermometer using oxide nanotubes (such as MgO, In_2O_3 and SiO_2) that has better thermal resistance and oxidation resistance than a carbon nanotube, and clarified its temperature reaction.

PUBLISHED RESEARCH PAPERS

1) YH.Gao and Y.Bando, "Carbon nanothermometer containing gallium", *Nature,* 415,599 (2002)
2) YB.Li, Y.Bando, et al, "Ga-filled single crystalline MgO nanotube:Wide-temperature range nanothermometer", *Appl. Phys. Lett,* 83, 999-1001 (2003)
3) YH.Gao, Y.Bando et al, "Temperature measurement using a gallium-filled carbon nanotube", *Appl. Phys. Lett,* 83, 2913-1915 (2003)
4) ZW.Liu, Y.Bando, et al, "Unusual freezing and melting of gallium encapsulated carbon nanotubes", *Appl. Phys. Lett,* 93, 095504 (2004)

ADDITIONAL INFORMATION ABOUT NANOTUBES

Iijima discovered the carbon nanotube in 1991. It is a new cylindrically shaped atomic sheet consisting of carbon rolled into a cylinder. A nanotube made of a single sheet is called a single-walled nanotube, while a nanotube made of multiple sheets is called a multi-walled nanotube. A nanotube ranges in size from one nanometer to tens of nanometers in diameter and about several microns long. Carbon nanotubes are expected to be used as field-emission display emitters, and probes for scanning probe microscopes, fuel cells, etc. A nanothermometer is an example of a new application of thermal sensor nanotubes. Known applications of non-carbon nanotubes other than carbon include BN and MoS_2.

INQUIRIES
Nanoscale Materials Center Yoshio Bando
E-mail : BANDO.Yoshio@nims.go.jp

6 Fabrication of Functional Materials Using Nanosheets as Building Blocks

■ EXECUTIVE SUMMARY

Two-dimensional crystallites with an extremely small thickness of ~1 nm and a lateral size of micrometers can be synthesized by exfoliating layered host compounds using soft-chemical procedures. The resulting nanosheets, e.g. titania nanosheets, can be used as a nanoscale "Lego block" to fabricate various nanostructured materials via wet processes. This approach allows the design of functionality of the materials, due to the precise control of nanoarchitecture and combination of nanosheets and their counterparts, such as functional organic molecules, metal complexes and inorganic cluster ions. We have demonstrated that a number of useful materials can be synthesized using this strategy.

■ OUTLINE

Nanosheets are obtained as a charged colloid dispersed in solvent (usually aqueous media).[1] The application of solution-phase processing leads to a range of materials with various nanostructures, textures and physicochemical properties.

One of the important techniques is flocculation, which involves mixing electrolytes with a colloidal suspension of nanosheets. The nanosheets are restacked into a wool-like precipitation (Figure 1), accommodating counter ions in the nanosheet gallery. This reaction provides a facile and versatile route to produce lamellar nanocomposites. In addition, products generally have a high surface area associated with porosity, which is advantageous for some applications.

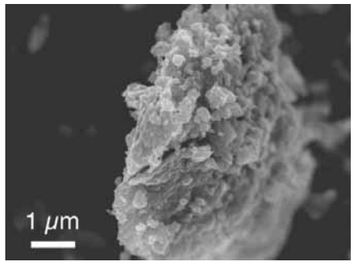

Fig. 1 SEM image of a flocculated product of nanosheets.

The nanosheets can be deposited laye-by-layer through electrostatic self-assembly to produce ultrathin films of nanosheets on various substrates. The film can be fabricated by repeatedly dipping the substrate into the colloidal suspension of the nanosheets and an aqueous polyelectrolyte solution (Figure 2).

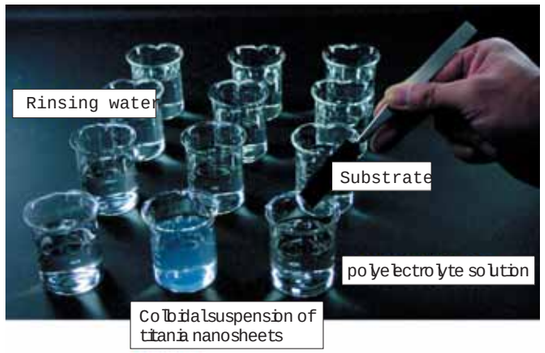

Fig. 2 Layer-by-layer nanosheet deposition procedures

Nanosheets and polyelectrolytes are alternately adsorbed in monolayers via electrostatic interaction, which enables wet-process coating with a thickness precision in the range of a nanometer. Furthermore, the nanosheets can be deposited onto non-flat surfaces thanks to their highly flexible nature. For example, hollow oxide nanoshells (Figure 3) can be fabricated by depositing the nanosheets on micron-sized polymer beads and the subsequent thermal decomposition of the core.

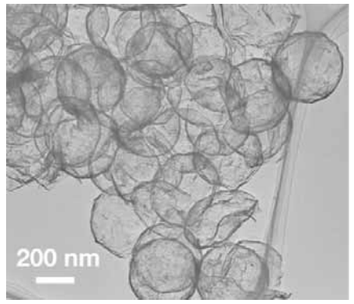

Fig. 3 TEM image of titania hollow nanoshells.

■ ACHIEVEMENTS

Semiconducting titania nanosheets were flocculated with rare earth ions, such as Eu^{3+}, to yield a lamellar nanocomposite, which exhibited photoluminescence properties when exposed to UV light, due to the efficient transfer of energy from the host to the rare earth ions.[2] Flocculation of titania or perovskite nanosheets produced photocatalysts in which nanoparticles of Pt or RuO_x were highly dispersed. These materials underwent total decomposition of water into H_2 and O_2 under UV irradiation.[3] We have also synthesized various useful materials through the flocculation process; a layered manganese oxide showing a stable electrochemical redox capability, and a novel porous material with a double-layer pillared structure.[4]

Multilayer ultrathin films of titanium and manganese oxide nanosheets were found to exhibit a high self-cleaning property, and efficient electrochromic behavior, respectively. These two different nanosheets could be assembled layer-by-layer into superlattice-like nanostructures, which show interesting photochemical reactivities. Furthermore, the complex nanoassemblies were constructed by combining nanosheets with various inorganic clusters and metal complexes. We also succeeded in fabricating hollow nanoshells of titanium and manganese oxides with the thickness of nanometers.[5]

PUBLISHED RESEARCH PAPERS

1) "Science and Applications of Inorganic Nanosheets", Edited by K. Kuroda and T.Sasaki,CMCPublication(2005).
2) H. Xin, R. Ma, L.Z. Wang, Y. Ebina, K. Takada and T. Sasaki: *Appl. Phys. Lett.* 85 (2004) 4187.
3) Y. Ebina, N. Sakai and T. Sasaki: *J. Phys. Chem. B* 109 (2005) 17212.
4) T. Tanaka, K. Fukuda,Y. Ebina, K. Takada and T. Sasaki: *Adv. Mater.* 16 (2004) 872.
5) L. Z. Wang, N. Sakai, Y. Ebina, K. Takada and T. Sasaki: *Chem. Mater.* 17 (2005) 1352.

ADDITIONAL INFORMATION ABOUT NANOSHEETS

There are a wide variety of layered host compounds, e.g. graphite and mica, in which two-dimensional layers are stacked. Nanosheets are a new class of nanoscale materials that are obtained via delamination of a layered compound into its elementary layers. The nanosheets have exceedingly high two-dimensional anisotropy; a very small thickness comparable to molecules versus a lateral size in micrometer scale. A number of layered hosts, ranging from clay minerals to chalcogenides, oxides and hydroxides, have been exfoliated into nanosheets. In particular, the success in synthesizing functional oxide nanosheets, such as titania or perovskite nanosheets and some novel physical properties, e.g. size quantization effects, have evoked strong interest in this fascinating class of nanomaterials.

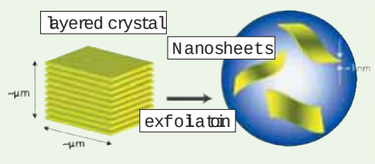

Schematic explanation of exfoliation

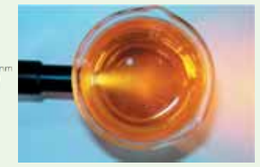
Suspension of MnO_2 nanosheets

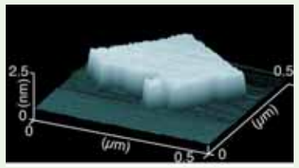

AFM image of $Ca_2Nb_3O_{10}$ nanosheet

INQUIRIES
Nanoscale Materials Center Takayoshi Sasaki
E-mail : SASAKI.Takayoshi@nims.go.jp

7 Development of Brightness and Highly efficient Sialon Phosphors

■ EXECUTIVE SUMMARY

Sialons, solid solutions of silicon nitride containing Si, Al, O, and N (Fig. 1), are ceramics that have been studied as heat-resistant materials. We have discovered that rare-earth doped sialons have strong photoluminescence, and then successfully developed them as highly efficient green, yellow and red phosphors. Sialon phosphors can be excited by blue LEDs efficiently, and have excellent durability and thermal stability, therefore, it is anticipated that they will be used as luminescent materials for white LEDs.

■ OUTLINE

Because white LEDs (light-emitting diodes) have outstanding environmental features, including low power consumption, long life, and they do not use mercury, it is expected that they will replace traditional fluorescent lamps for general lighting in the near future. It is essential that the phosphors for white LEDs can be excited by blue light, and it is required that they should have high durability when irradiated by strong light for long periods of time. Current phosphors are predominately based on oxide or sulfide hosts and only a few of them can be excited by visible light. These phosphors also have low durability. Sialon or silicon nitride-based materials have long been studied as heat-resistant ceramics at NIMS. Recently, we have suggested new concept phosphors based on sialon hosts, and succeeded in the synthesis of highly efficient sialon phosphors possessing excellent thermal and chemical stability (Fig. 2).

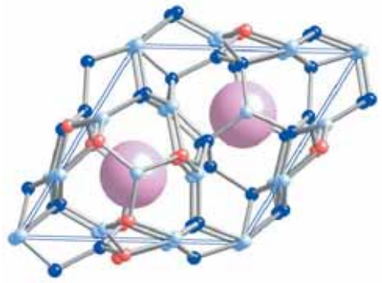

Fig.1 Crystal structure of sialon.

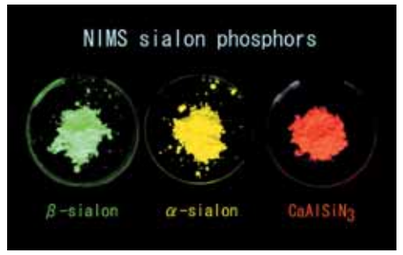

Fig.2 Developed sialon phosphors.

Sialon phosphors are prepared by mixing the raw powders of silicon nitride (Si_3N_4), aluminum nitride (AlN), calcium carbonate ($CaCO_3$), europium oxide (Eu_2O_3), and firing at 1700 – 2000℃ in a 10 atm N_2 atmosphere.

The sialon phosphors are superior to their oxide counterparts in the following aspects:

(1) High durability: The host crystals are mainly developed as structural or heat-resistant materials, and they are chemically stable. These phosphors are especially suitable for LEDs that are exposed to long-term high-energy excitation light.

(2) Small thermal quenching: The strong chemical bonding in sialons means temperature enables small changes in emission efficiency. An important feature of the LEDs is that the temperature varies during operation.

(3) Visible-light excitable: The introduction of nitrogen increases the covalency of the chemical bonds in sialons, which allows for longer wavelength excitation/emission of sialon phosphors compared to oxide phosphors. It is thus able to obtain phosphors for white LEDs that can be excited efficiently by a blue LED with a primary emission wavelength of 450 nm.

(4) Great flexibility in materials design: As a solid solution, it is possible for sialons to have a broad range of composition, which makes it possible to tune the excitation/emission wavelength.

■ ACHIEVEMENTS

The yellow phosphor, Eu-doped a-sialon, was made in 2002 (center, Fig.2)[1]. The novel green β-sialon (left, Fig. 2)[2] and red $CaAlSiN_3$ (right, Fig.2)[3] phosphors were later developed successfully due to a detailed investigation of the crystal structure and composition of sialon-based ceramics. These phosphors are based on sialon crystals containing Si, Al, O, and N, the structures of which feature a small amount of Eu^{2+} ions dissolving at a specific part in the crystals. Variations in the environment surrounding Eu^{2+} in different crystals allow the sialon phosphors to emit different colors.

The developed sialon phosphors can be excited efficiently by blue LEDs with a primary emission of 450 nm, which qualifies them for use in white LEDs. Therefore, attempts have been made to create white LEDs with varied color temperatures by changing the blending ratio of three phosphors and the coating amount (Fig.3)[4]. The natural lighting source has been achieved, the color rendering index is as high as 82 – 88 and is superior to that of currently available white LEDs and fluorescence lamps.

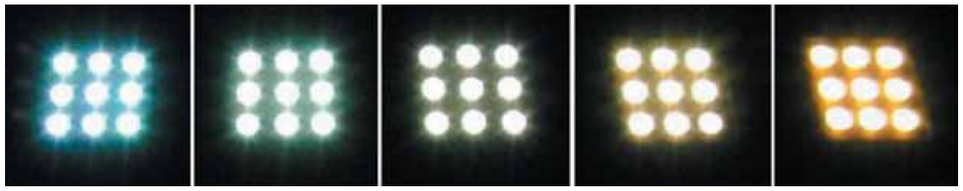

Fig.3 White LEDs using the developed red, green and yellows phosphors.
@ @ The color temperature varies continuously with changes in the blending ratio.

PUBLISHED RESEARCH PAPERS

1) R.-J. Xie, *et al., J. Am. Ceram. Soc.,* 85 [5] 1229-1234 (2002).
2) N. Hirosaki, *et al., Appl. Phys. Lett.,* 86, 211905 (2005).
3) K. Uheda, *et al., Electrochem. Solid-State Lett.,* 9 [4] H22-H25 (2006).
4) K. Sakuma, *et al., IEEE Trans. Electron,* E88-C [11] 2057-2064 (2005).

ADDITIONAL INFORMATION ABOUT PHOSPHORS

Do you think that you have seen phosphors HWhen you get home from work, turn on the light and switch on the television. What you see, such as the fluorescent light and images on the television, is light emitted by phosphors. We are living in a world surrounded by light from phosphors, although we do not pay much attention to it in daily life.

The styles for the illumination and display, both of which are indispensable in life, are changing greatly. Lighting is shifting from fluorescent lamps to white LEDs, and displays from CRTs to thin flat panels. For these new styles, high-performance and high-durability phosphors are essential. As next-generation luminescent materials, sialon phosphors meet the requirements of these trends.

INQUIRIES
Nano Ceramics Center Naoto Hirosaki
E-mail :HIROSAKI.Naoto@nims.go.jp

8 Cobalt Oxyhydrate Superconductors

■ EXECUTIVE SUMMARY

The cobalt oxyhydrate superconductor was discovered through interdisciplinary chemistry and physics research [1]. It is the first ever cobalt oxide superconductor and a special methodology called "soft chemistry" plays an important role in its synthesis. Its superconducting transition temperature (T_c) is 4.6 K, which is much smaller than T_c's of cuprate superconductors. This compound has fascinated both chemists and physicists, so the first superconductor[1] report has been cited more than 350 times. It is expected that a basic understanding of this superconductor will help to clarify the mechanism of high T_c superconductivity in cuprates.

■ OUTLINE

Since the discovery of high T_c superconductivity in copper oxide systems in 1986, efforts have been made to explore similar effects on oxide systems of nickel and cobalt (located near copper on the periodic table). However, such attempts have always failed and there was a general consensus that copper is a key element for superconductivity. Thus, the discovery of the cobalt oxyhydrate superconductor at NIMS surprised many researchers.

In the preparation of this compound[1], γ-$Na_{0.7}CoO_2$ is first synthesized by a conventional solid-state reaction and its Na atoms are then partially deintercalated by Br_2 in an acetonitrile solution. The sample is then immersed in distilled water so that water molecules are intercalated between the CoO_2 layers (Fig.1). The oxyhydrate thus obtained has a strong two-dimensional structure with a doubled CoO_2-CoO_2 layer distance, compared to the original γ-$Na_{0.7}CoO_2$ material. As shown in Fig.2, this oxyhydrate (approximate composition $Na_xCoO_2yH_2O$) is categorized as an "extreme" type Ⅱ with T_c=4.6 K and a high upper critical field. It is clear from the aforementioned synthesis process that soft chemical procedures are indispensable in the preparation of this unique superconductor.

Recent research at NIMS[2] has clarified that the hydration process is not simple, i.e. the Na^+ ions are substituted by oxonium ions (H_3O^+) during hydration, resulting in the composition of Nax $(H_3O)_zCoO_2 \cdot yH_2O$ (typical values are x ≈ 0.35, z ≈ 0.16, y ≈ 1.14).

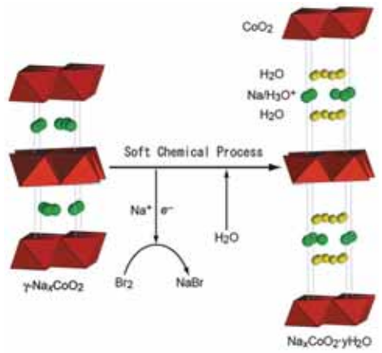

Fig.1 Crystal structure and synthesis process of the cobalt oxyhydrate superconductor

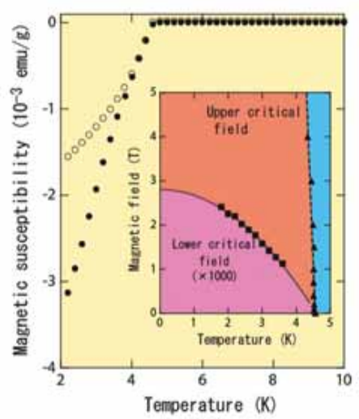

Fig.2 Magnetic susceptibility and upper and lower critical fields of the cobalt oxyhydrate superconductor.

Moreover, varying the ratio of Na^+ and H_3O^+ (z/x) and keeping the Co valence constant[3] creates the superconducting phase diagram. Surprisingly, in the resulting phase diagram (Fig.3), superconductivity appears in two different areas divided by a non-superconducting phase. This non-superconducting phase is a magnetic phase with a long-range magnetic ordering near 6 K and has been recognized by nuclear quadrupole resonance (NQR) experiments.

The phase diagram is quite important because it indicates that the non-superconducting magnetic phase exists just next to the superconducting phases, and drastic transformation between superconducting and magnetic phases is induced by the substitution of Na^+ with H_3O^+ (i.e. without addition or subtraction of carriers). This diagram suggests a strong non-conventional superconductivity mechanism with magnetic origins.

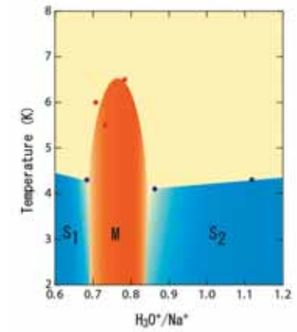

Fig.3 Superconducting phase diagram of Nax$(H_3O)_zCoO_2 \cdot yH_2O$ drawn for the parameter of H_3O^+/Na^+ keeping the cobalt valence at +3.4. S_1 and S_2 denote the superconducting phases, and M the non-superconducting magnetic phase.

■ ACHIEVEMENTS

(1) The first cobalt oxide superconductor was discovered by utilizing soft chemical processes.
(2) The exact chemical composition of the superconductor was defined as Na_x $(H_3O)_zCoO_2 \cdot yH_2O$ and its crystal structure was analyzed accurately.
(3) The superconducting phase diagram was made by varying the ratio of Na^+ and H_3O^+ (z/x), keeping the Co valence constant and it was found for the first time that a non-superconducting magnetic phase exists just next to the superconducting phases in the diagram.

PUBLISHED RESEARCH PAPERS

1) K. Takada, H. Sakurai, E. Takayama-Muromachi, F.Izumi, R. A. Dilanian, and T. Sasaki, *Nature* 422 (2003) 53-55.
2) K. Takada, K. Fukuda, M. Osada, I. Nakai, F. Izumi, R. A. Dilanian, K. Kato, M. Takata, H. Sakurai, E. Takayama-Muromachi and T.Sasaki, *J. Mater. Chem.* 14 (2004) 1448-1453.
3) H. Sakurai, K. Takada, T. Sasaki and E. Takayama-Muromachi, *J. Phys. Soc. Jpn*. 74 (2005) 2909-2912.

ADDITIONAL INFORMATION ABOUT SUPERCONDUCTIVITY

Dutch physicist Kamerlingh Onnes discovered superconductivity in 1911. He measured mercury's electric resistivity at a very low temperature and found that it decreased steeply and was zero below 4.2 K. He termed this phenomenon superconductivity. The most easily understandable properties of superconductivity are the complete absence of electric resistivity (perfect conductivity), and its unique magnetic phenomenon. Suppose that a magnetic field is induced in a material in its normal state, and the material is then cooled and transformed to a superconducting state. It was found that in the superconducting state thus obtained, the magnetic fluxes were completely pushed out of the material. This perfect diamagnetism, which occurs independently of magnetic history, cannot be explained by perfect conductivity, and thus is an independent phenomenon called the Meissner effect.

INQUIRIES
Advanced Nanomaterials Laboratry Eiji Muromachi
E-mail : MUROMACHI.Eiji@nims.go.jp

9 High-Strain-Rate Superplastic Ceramics

■ EXECUTIVE SUMMARY

This project developed oxide ceramics that exhibit high strain rate superplasticity (HSRS) of 10^{-1} - 10^{0} s^{-1} and large tensile ductility that range from 200 to 2500 %, in a collaboration of studies on superplasticity and processing science. The calibration also brought about a guide to microstructural control for attaining HSRS in oxide ceramics. The obtained materials and the guide are expected to pave the way for industrial net-shaping of oxide ceramics.

■ OUTLINE

The discovery of superplasticity in tetragonal zirconia has provided an attractive route for net-shape forming or joining of ceramic materials. Industrial applications, however, are still highly limited. This situation is mainly due to the low strain rate available to superplastic forming: superplasticity in most ceramics occurs at 10^{-5} - 10^{-4} s^{-1}. At a strain rate of 10^{-4} s^{-1}, it takes about 3 hours to elongate a material with an initial length of 10 mm to a final length of 20 mm (Fig. 1) and such forming time is unattractive in industry. The deformation is drastically reduced to 2 minutes or less when the material is deformable at $\geqq 10^{-2}$ s^{-1}. In metallic materials, superplasticity at 10^{-2} s^{-1}, namely the high strain rate superplasticity (HSRS), has been a key in commercial net-shaping and should be applicable also in the ceramic materials.

Strain Rate (s^{-1})	Forming Time
10^{-4}	170 min. (3h)
10^{-2}	100 sec.
10^{-1}	10 sec.
10^{0}	1 sec.

Fig.1 Estimation of forming time.

Fig.2 Collaboration between (a) deformation and failure mechanisms and (b) processing science that leads to (c) microstructural design for attaining high strain rate superplasticity.

The close collaboration between studies on superplastic deformation and relating phenomena, such as intergranular cavitation and dynamic grain growth and studies on the processing dependence of the former issues, derived a microstructural guide for attaining HSRS in oxide ceramics (Fig.2). We also established processing methods to obtain fine-grained homogeneous microstructures that meet the guidelines (Fig.2).

■ ACHIEVEMENTS

Using the guide and the processing methods, we attained HSRS at 10^{-1} - 100 s^{-1} in Al_2O_3-ZrO_2-MgO・Al_2O_3 spinel (Fig. 3, as it appears in Nature) and at 10^{-2} - 10^{-1} s^{-1} in ZrO_2 dispersed with $MgAl_2O_4$. The former material exhibited a highly enhanced tensile ductility of 2500% at 10^{-1} s^{-1} (Fig.3). We also attained HSRS with tensile ductility larger than 200% at relatively low temperatures of 1350 - 1450 ℃ in monolithic tetragonal zirconia (3Y) doped or co-doped with Al_2O_3, TiO_2-MgO, or Al_2O_3-Mn_2O_3.

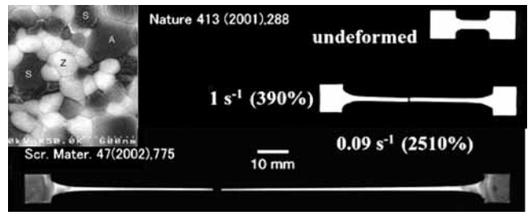

Fig.3 High strain rate superplasticity and large tensile ductility attained in Al_2O_3-ZrO_2-MgO・Al_2O_3 spinel. The upper-left figure shows the as-sintered microstructure.

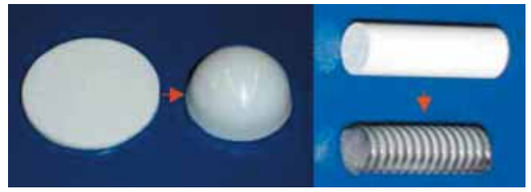

Fig.4 Net-shaping of a zirconia that exhibits high strainrate superplasticity.

The current results show that HSRS can intentionally be attained in oxide ceramics. The microstructural guide, the established processing methods and the developed materials are expected to be a breakthrough for industrial applications of superplastic net-shaping (Fig.4) and joining of ceramic materials.

PUBLISHED RESEARCH PAPERS

1) B.-N. Kim, K. Hiraga, K. Morita and Y. Sakka: *Nature* 413 (2001) 288.
2) K. Morita, K. Hiraga, B.-N. Kim and Y. Sakka: *J. Am. Ceram. Soc.* 85 (2002) 1900.
3) K. Hiraga, B.-N. Kim, K. Morita, T. S. Suzuki, Y. Sakka: *J. Ceram. Soc. Jpn.* 113 (2005) 191.
4) Japanese Patent 3350710, "Alumina-base Superplastic Ceramics" 20. 9. 2002.

ADDITIONAL INFORMATION ABOUT SUPERPLASTICITY IN CERAMIC MATERIALS

Superplasticity is defined as a material's ability to sustain large tensile elongation and had been regarded as a phenomenon appearing only in fine-grained metallic materials. In 1986, however, this ability was also found in a tetragonal zirconia (Wakai et al.). This was followed by the discovery of superplasticity in other oxide and nitride materials.

Superplasticity has been expected to bring about an innovation in the shaping of ceramics, since plastic shaping enables us to cut the high cost of grinding and polishing the rigid materials. Bypassing grinding should heighten the post-forming strength at room temperature, which is highly sensitive to fine flaws introduced by grinding. In addition, the high-temperature strength of the shaped product can be heightened by a post-forming heat treatment that increases the grain size of the material. Metal-like formability at high temperatures and strength and hardness at room temperature are thus possible in superplastic ceramics. For industrial applications, the keys are plastic-forming technologies adequate for ceramic materials and high strain rate superplasticity.

INQUIRIES
Nano Ceramics Center Keijiro Hiraga
URL: www.http://nims.go.jp/kouyuuten/index_e.html
E-mail: HIRAGA.keijiro@nims.go.jp

10 High-purity hBN Single Crystal and Ultraviolet Light Emission

■ EXECUTIVE SUMMARY

Boron nitride (BN) occupies the first period of groups Ⅲ and Ⅴ in the periodic table of elements. Similar to AlN and GaN of Ⅲ-Ⅴ compounds, BN has attractive potential as a wide band-gap material. However, high-purity single crystalline BN was yet to be obtained, and its characteristics were unknown so far. In recent,the promising semiconductor characteristic (direct band-gap: 5.97 eV) was discovered from high-purity hexagonal boron nitride (hBN) crystals obtained by a high-pressure flux method, paving the way for a new and efficient, deep ultraviolet emission material.

■ OUTLINE

Developing a semiconductor light-emitting device with a short wavelength below 300 nm is a very important technical challenge, not only for technical innovation for information storage, but also for responding to new demands for environmental preservation, such as sterilization materials which substitute for mercury lamps. In order to obtain efficient deep ultraviolet light emission from a semiconductor, it is necessary to use a direct wide band-gap semiconductor with high crystal quality with few defects that cause disturbance and reduce the emission efficiency. Therefore, materials that can be used as deep ultraviolet emission materials are limited. Research is now heading toward breakthroughs that will improve the properties of conventional semiconducting materials, such as electric conductivity control and reduction of crystal defects, and also the search for a new candidate with attractive efficient light emission potential.

Hexagonal BN (hBN) and cubic BN (cBN) are known as the representative crystal structures of BN. Hexagonal BN is chemically and thermally stable, and has been widely used as an electrical insulator and heat-resistant material for many years. cBN, which is a high-density phase, is an ultra-hard material next to diamond. In practical applications, it is indispensable for tools used in machining ferrous metal materials.

NIMS has been conducting the synthesis study of super-hard materials, which includes cBN and diamonds. cBN has the attractive potential of a super-hard material, as well as the largest band-gap of 6.3 eV among the Ⅲ-Ⅴ group compounds. Recently we synthesized high-purity single cBN and hBN crystals under high pressure, and succeeded in educing interesting properties in hBN single crystals as a result of the reduced concentration of impurities, such as oxygen and carbon.

Thus far, it has not been possible to obtain single, good quality hBN crystals that are suitable for various evaluations and, particularly, research focusing on light-emitting properties has been inadequate. The high-purity single crystalline hBN displays a clear hexagonal idiomorphology, and is colorless and has high transparency (Fig.1). When the optical properties of these crystals were evaluated, a high intensity cathodoluminescence (CL) peak was observed, as shown in Fig.1.

From the observed optical characteristics, hBN is a semiconductor of the direct band-gap of 5.9 eV. It has thus been proven that hBN has excellent potential as a candidate for a new deep ultraviolet light emission element.

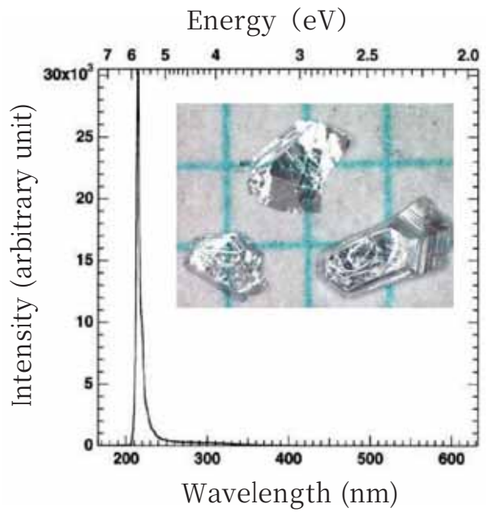

Fig.1 Optical microscopic photograph of single crystalline hBN and CL spectrum.

■ ACHIEVEMENTS

Although hBN has a lamellar structure, when parallel plate-shaped hBN crystals were cut by cleavage, and the crystals were excited by irradiation with an electron beam, it was found that emission wavelengths of 215 nm caused several phenomena that are characteristic with laser operation, confirming room temperature lasing (Fig. 2) [1].

This new discovery revealed that hBN possesses direct wide band-gap semiconductor (Eg: 5.97 eV) properties.[2),3)] Control of electrical conductivity in order to realize high efficiency UV emissions will be an important challenge for the future. However, even at present, this material can be used with various kinds of high performance electron-emitting devices. For example, easy construction of compact DUV-emitting devices for wavelengths around 215 nm can be expected by combining this hBN material with diamonds, carbon nanotubes, or other cold cathode device materials.

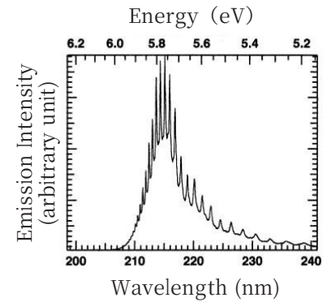

Fig.2 Spectrum of room temperature laser generation by excited electron beam of hBN.

PUBLISHED RESEARCH PAPERS

1) K.Watanabe, T.Taniguchi and H.Kanda, *Nature Materials,* 3, (2004) 404.
2) T. Taniguchi, K. Watanabe, A, Nakayama: The Science and Technology of High Pressure, 15(4)(2005) 284
3) Official Gazette, TOKUKAI No. 2005-145789

ADDITIONAL INFORMATION ABOUT HEXAGONAL-CRYSTALLINE BORON NITRIDE (hBN) MATERIALS WITH NEW FUNCTIONALITIES

The crystal structure of hBN is composed of stacks of two-dimensional chicken-wire layers of boron and nitrogen atoms. It has excellent chemical stability, heat resistance, and high electric insulation, as well as good lubrication effects arising from its layer structure. Therefore, there is a wide field of application, such as solid lubrication, mold lubrication, heat insulation materials, insulators, crucibles and so forth.

As for hBN synthesis, various methods, such as a reduction nitriding reaction of boron oxide and a vapor phase deposition, are applied for the desired application and shape. While there have been several reports of studies focusing on hBN's optical properties, its intrinsic nature has not been well clarified, probably due to the lack of high-purity single crystals.

This study has shown the attractive potential of hBN as a wide-gap semiconductor by evaluating the optical characteristics using a high-purity single crystal. Although the study of optical characteristics attributed to the unique layer structure is still in the early stage in the development, hBN is a new material that will attract further research.

INQUIRIES
Advanced Nanomaterials Laboratory Takashi Taniguchi
Optical Material Center Kenji Watanabe
E-mail : TANIGUCHI.Takashi@nims.go.jp
WATANABE.Kenji.aml@nims.go.jp

11 $Sm(Co,Cu)_5$/FeCo anisotropic nanocomposite film

■ EXECUTIVE SUMMARY

To explore the possibility of developing high performance nanocomposite permanent magnets, anisotropic $[Sm(Co,Cu)_5/FeCo]_6$ nanocompsite multilayer thin films were fabricated by the magnetron sputtering technique. A strongly exchange coupled nanocomposite film exhibited strong in-plane anisotropy with maximum energy product of 32 MGOe. This energy product is higher than the theoretical limit for the $SmCo_5$ single phase magnets, demonstrating that higher perfomance permanet magnets can be produced if ideal inisotropic soft/hard nanocomposite structure can be achieved.

■ OUTLINE

Nanocomposite magnets, composed of exchange coupled hard and soft magnetic phases, have been the subject of recent studies regarding their potential to achieve the maximum energy product $(BH)_{max}$ higher than that achieved by existing sintered magnets Although various types of nanocomposite magnets were reported in the Nd-Fe-B system, their coercivity (H_c), remanence (B_r), and $(BH)_{max}$ were lower than those of commercial sintered magnets of the same system due to their isotropic feature; thus, nanocomposite magnets are now considered as economical medium-performance materials for bonded magnet applications. However, crystallographically textured anisotropic nanocomposites still have great technological potential to achieve a higher $(BH)_{max}$. Since many complicated metallurgical processes are involved in producing anisotropic bulk nanocomposites, textured multilayer thin films serve as a convenient model system for studying the fundamental properties of exchange-spring magnets. Calculations by Skomski and Coey[1] predicted that the upper limit of $(BH)_{max}$ for anisotropic $Sm_2Fe_{17}N_3/Fe_{65}Co_{35}$ multilayers, with a volume fraction of only 9% of the hard phase, was 137MGOe. Thus, an experimental demonstration of high $(BH)_{max}$ achievable by an anisotropic multilayer exchange coupled magnet will boost the research toward new high performance permanent magnetic materials. In this work, we selected $SmCo_5$ with a huge magnetocrystalline anisotropy K_u (K_u>108 erg/cc) as a hard phase and Fe as a soft phase. In previous investigations[2),3)], textured multilayers were fabricated by depositing the Sm-Co and Fe or Co layers onto a heated substrate or by directly depositing the layers at room temperature, and the reported $(BH)_{max}$ was only in the range of 10 to 20GMOe. In this work, we succeeded in fabricating well textured $Sm(Co,Cu)_5$/Fe multilayer films by sputtering and subsequent annealing. After the post-annealing, the multilayer structure was kept with a good in-plane c-axis texture. A high $(BH)_{max}$ of 32GMOe was obtained, which is larger than that achieved in the $SmCo_5$ and $Sm(Co,Fe,Cu,Zr)_7$ type commercial sintered magnets.

■ ACHIEVEMENTS

The multilayer films were prepared by sequentially depositing Sm-Co, Cu, and Fe layers on a 100 nm thick Cr underlayer that was sputter deposited on a thermally oxidized Si wafer. The reason for adding the Cu interlayers is that it is immiscible with Fe, but can dissolve in the Sm-Co layer. The Sm-Co layers with a nominal composition of $SmCo_6$ were deposited by co-sputtering Sm and Co targets. After depositing the multilayer films, a 50 nm thick Cr capping layer was deposited to protect the oxidation of the films. The structure of the Sm-Co layer was amorphous in the as-deposited condition, so the as-deposited films were Cr(50nm)/[*a*-(Sm-Co) (9nm)/Cu (*x*nm)/Fe (5nm)/Cu (*x*nm)]6/Cr (100nm)/*a*-SiO_2, where *a*- stands for amorphous. The films were then heat-treated at temperatures ranging from 450℃ to 525℃ for 30 min.

As shown in Fig. 1, we have successfully fabricated the exchange coupled $[Sm(Co,Cu)_5/Fe]_6$ multilayer films by post-annealing the Cr(50nm)/[*a*-(Sm-Co) (9nm)/Cu (0.5nm)/Fe (5nm)/Cu (0.5nm)]6/Cr (100nm)/*a*-SiO_2 multilayers. The addition of the Cu interlayers between the *a*-Sm-Co and Fe layers with an appropriate thickness improved the coercivity and $(BH)_{max}$, especially at low annealing temperatures. This is related to the reduced crystallization temperature of the amorphous Sm-Co phase, as well as the substitution of Cu for Co to form the $Sm(Co,Cu)_5$ phase. The largest $(BH)_{max}$ was 32 MGOe, which is larger than the theoretical limit for a $SmCo_5$ single phase magnet, 28.8 MGOe. This value is also larger than those of the commercial $SmCo_5$ and $Sm(Co,Fe,Cu,Zr)_7$ type sintered magnets. By replacing Fe with $Fe_{65}Co_{35}$ or adjusting the thickness of hard and soft layers, it will be possible to enhance the $(BH)_{max}$ further. This work has demonstrated that there is the potential to develop high performance exchange spring magnets by fabricating strong exchange coupled anisotropic soft and hard phase nanocomposites.

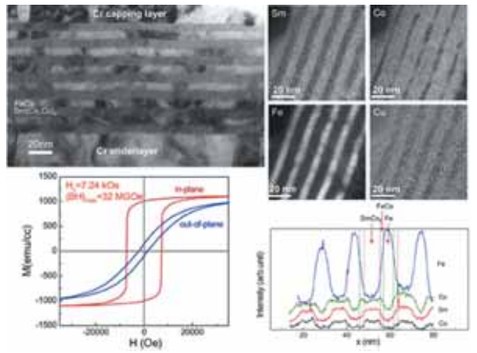

Fig.1 (a) Cross sectional TEM image of $[Sm(Co,Cu)_5/FeCo]_5$ multilayer thin film and (b) in-plane and out-of-plane magnetization curves. The in-plane coercivity is 7.24 KOe and (BH)max=32 MGOe, which is larger than the theoretical limit for a $SmCo_5$ single phase magnet (29 MGOe). (c) GIF elemental mapping of Sm, Co, Fe, Cu and the intensity profile obtained from the GIF mapping. Cu interlayer initially sandwiched between a-$SmCo_6$ and Fe diffuse into the $SmCo_5$ phase forming $Sm(Co,Cu)_5$ and the excess Co in the a-$SmCo_6$ phase diffuse in the Fe layer.

REFERENCES

1) R. Skomski and J. M. D. Coey, *Phys. Rev. B* 48, 15812 (1993).
2) E. E. Fullerton, J. S. Jiang, C. H. Sowers, J. E. Pearson, and S. D. Bader, *Appl. Phys. Lett.* 72, 380 (1998)
3) E. E. Fullerton, J. S. Jiang, M. Grimsditch, C. H. Sowers, and S. D. Bader, *Phys. Rev. B* 58, 12193 (1998).

PUBLISHED RESEARCH PAPERS

"Sm(Co,Cu)5/Fe exchange spring multilayer films with high energy product", J. Zhang, Y. K. Takahashi, R. Gopalan, and K. Hono, *Appl. Phys. Lett.* 86, 122509 (2005) .

ADDITIONAL INFORMATION ABOUT NANOCOMPOSITE MAGNETS

This work has experimentally demonstrated that an anisotropy exchange coupled soft/hard nanocomposite can lead to the energy product that is larger than the theoretical limit for a single phase magnets. Since the saturation magnetization of the $SmCo_5$ phse is not as large as that of $Nd_2Fe_{14}B$, the maximum energy product was only 32 MGOe. However, this work suggests that it will be possible to break the current record of high energy product, 55 MGOe, if high coercive anisotropic nanocomposite of $Nd_2Fe_{14}B$/FeCo can be successfuly fabricated,. Since the theoretical limit for the $Nd_2Fe_{14}B$ phase is 64 MGOe, the energy product exceeding 64 MGOe could be possible by fabricating an anisotropic $Nd_2Fe_{14}B$/FeCo nanocomposite.

INQUIRIES
Magnetic Material Center Kazuhiro Hono Yukiko Takahashi
URL: http://www.nims.go.jp/apfim
E-mail: KAZUHIRO.Hono@nims.go.jp

12 Development of Frequency Conversion Devices Using Ferroelectric Polarization Engineering

■ EXECUTIVE SUMMARY

Lithium niobate ($LiNbO_3$; LN in abbreviation) and lithium tantalate ($LiTaO_3$;LT) are typical ferroelectric materials used as single crystals. They are well known as materials containing huge numbers of intrinsic lattice defects (non-stoichiometric defects) in conventional crystals due to conventional crystal growth methods. In NIMS, we invented a single crystal growth method using a double crucible (see ADDITIONAL INFORMATION) in order to reduce the defect densities by more than one order of magnitude. Using these defect-controlled crystals, we discovered a dramatic reduction in the electric field required for the ferroelectric polarization inversion (coercive field). This reduction in the coercive field contributes to the development of frequency conversion devices with ferroelectric polarization engineered structures, which can be applied to conversions of fundamental laser light from UV to IR wavelength light.

■ OUTLINE

Expansion of available wavelengths by frequency conversion from semiconductor lasers and solid-state lasers is an emergent subject of research in nonlinear optics because the available wavelength from compact and maintenance free lasers is still limited.

Recently, frequency conversion, using ferroelectric crystals with periodical polarization structures that can be widely used in nonlinear optics applications based on the quasi-phase-matching (QPM) technique, has received a lot of attention. QPM offers tremendous advantages in utilizing the largest nonlinear coefficients with non-critical phase matching within the wavelength transparency range of the crystals. LN and LT crystals are the most attractive materials for QPM devices due to their large nonlinear and electro-optic coefficient. QPM requires the engineering of periodical polarization structures, so that the magnitude of the coercive field (the electrical field required to inverse polarization) becomes essential for fabricating devices.

By using the defect-controlled stoichiometric LT (SLT) crystals with 10 times larger frequency conversion efficiency than conventional nonlinear optical crystals, we can use a compact fundamental laser with ten times less power for the generation of the same power. When such a small laser is used, the heat generation can be suppressed and no water cooling system is necessary. It is very significant technology that enables to realize a small and stable frequency conversion system. Moreover, MgO-doped SLT crystals have the advantage of almost zero photorefractive damage, which guarantees frequency conversion even at room temperature with high beam quality.

NIMS original stoichiometric LN and LT (SLN and SLT) exhibit a much smaller coercive field for polarization inversion by 1/5 ~ 1/13. This makes the fabrication of devices much easier compared with the conventional materials. In addition, it was discovered that the thermal conductivity of defect-controlled crystals is more than twice as large as those of conventional crystals. The high thermal conductivity is of great significance when the heat generation at high power operation is taken into account. NIMS has already announced a high efficient frequency conversion prototype device for OPO from 1500 nm to 4500 nm wavelengths light from 1064 nm fundamental laser light, and SHG devices for 488 nm (Fig.1) and 532 nm light generation (Fig.2). Such devices can be applied to medical treatments, diagnosis, environment monitoring, laser displays etc.

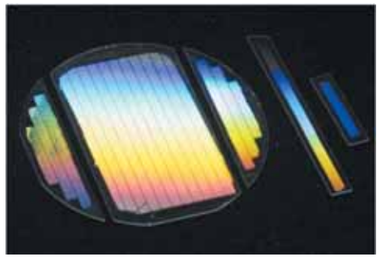

Fig.1 Stoichiometric LT wafer (2 inch diameter) with periodical polarization structure fabricated for second harmonic generation of 488 nm light converted from 997 nm fundamental laser light.

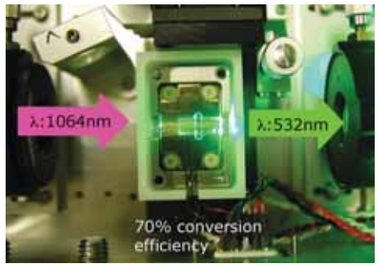

Fig.2 Second harmonic generation for 532 nm green light using stoichiometric LT with periodical polarization structure. Fundamental laser of 1064 nm wavelength is used.

■ ACHIEVEMENTS

(1) We succeeded in fabricating bulky optical parametric oscillation devices using stoichiometric LT crystals developed in NIMS. The device is over 2 mm in thickness and 40 mm in length. On average, it generates mid IR laser light of more than 10W.
(2) We succeeded in developing second harmonic generation devices converting 1064 nm wavelength light into 532 nm green light. We achieved an output intensity of 5W operating at room temperature and 70% conversion efficiency by a single pass of fundamental light.
(3) We simulated heat generation models that can demonstrate how the heat is generated during the second harmonic generation in quasi-phase-matching devices. The simulation was proved to be consistent with the experimental results.

PUBLISHED RESEARCH PAPERS

1) NE. Yu, S. Kurimura, Y. Nomura, M. Nakamura, K. Kitamura, *Appl.Phys.Lett.,* 85,(2004) 5134
2) N.E.Yu, S.Kurimura and K.Kitamura; *Jpn.J.Appl.Phys.,* 42 (2003) 821.
3) O.A. Louchev, NE. Yu, S. Kurimura, K. Kitamura, *J. Appl. Phys.*98,(2005) 113103
4) O.A. Louchev, NE. Yu, S. Kurimura, K. Kitamura, *Appl. Phys. Lett.*, 87,(2005) 1131101

ADDITIONAL INFORMATION ABOUT GROWTH METHOD FOR SINGLE CRYSTALS WITH REDUCED DEFECT DENSITIES

There are single crystals which cannot realize its potential enough for practical usages although it presents excellent optoelectronic or nonlinear optical properties. Many kinds of single crystals cannot demonstrate their excellent potential because of impurities, defects, or inhomogeneity introduced into the crystals during their growth. Due to restrictions in conventional growth methods, there are many materials that cannot be grown with homogeneous compositions.

In NIMS, we succeeded in developing a novel method for growing high quality single crystals with low defect densities. The method is called the “double crucible Czochralski method”, where a crucible of double chamber structures is used, and powder with the same composition and the same amount of crystal growing from the melt is continuously supplied to the melt by an automatic system. This method has enabled crystal growth under defect-control by keeping the growth conditions constant and it is contributing to improvements in various properties of ferroelectric single crystals.

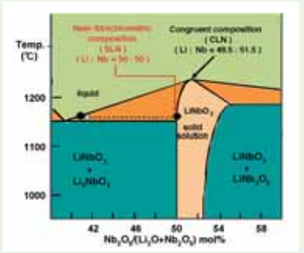

Schematic phase diagram of peudobinary system, Li_2O-Nb_2O_5 in the vicinity of $LiNbO_3$. phase[2.6].

Growth of single crystal under defectcontrol by double crucible method developed in NIMS.

INQUIRIES
Optronic Materials Center Kenji Kitamura
E-mail : KITAMURA.Kenji@nims.go.jp

13 Highly Tissue Compatible Artificial Bone Material

■ EXECUTIVE SUMMARY

To achieve early bone bonding, long-term stability and functionality, the artificial bone should satisfy the following requirements:
① High porosity ② High interconnectivity of pores ③ Suitable pore diameter for cell/tissue ingrowth ④ Sufficient mechanical strength for operations, even with high porosity.
To satisfy these requirements, we developed a strong, highly interconnective, high porosity artificial bone through the foaming of hydroxyapatite slurry and fixation of pores, and put it into practical use in the medical field.

■ OUTLINE

Porous bodies of calcium phosphates, such as hydroxyapatite (HAp), are practically used in the medical and dental fields due to their high osteocompatibility, i.e. direct bone bonding property. Conventional preparation procedures for porous bodies for artificial bones are as follows:
1. Impregnation of raw slurry into polymer foam, then burn the foam during sintering (template method)
2. Mix the raw materials with polymer beads, mold and burn the beads during sintering (polymer beads method)
3. Foaming raw material slurry and sintering.

However, these procedures cause problems for the mechanical strength and structure of artificial bones. From the viewpoint of strength, 1 and 2 can not inhabit formation of cracks, because 1 and 2 need to burn the polymers. That is, the thermal expansion of polymers and gases originates from the burning of polymers, which destructs pore walls composed of ceramics, and thus it is very difficult to increase mechanical strength. From a structural point of view, an increase in the interconnection path diameter is very difficult in 2 because it depends on contact faces between the beads. The fusion of pores during the drying process generally observed in 3 cause heterogeneity of the pore structure and decreases in interconnectivity.

We apply a water-soluble polymer that has good wettability to HAp for slurry formation reagent, and introduce crosslinks to the polymer to correct the pore structure. This inhibits the fusion of pores during the drying process, and we succeeded in developing an artificial bone with homogeneous pore structure, high interconnective pores, high porosity and a high level of mechanical strength.

Moreover, we proved the efficiency of novel material for the artificial bone and bone tissue scaffold due to its cell and tissue ingrowth properties in collaboration with Osaka University and AIST. Using these results, in a joint effort between private companies and NIMS, we promoted and commercialized the novel material for practical use as an artificial bone.

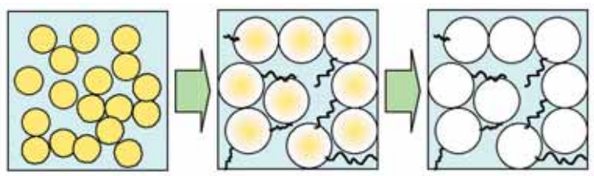

Example for 1 and 2 : Polymer expansion leads to crack formation.

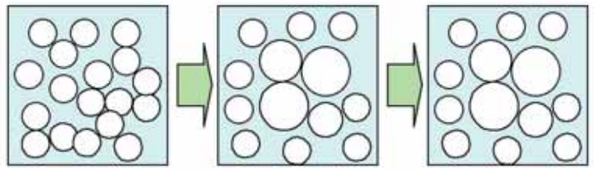

Example for 3 : Heterogeneous structure due to pore fusion during the drying process.

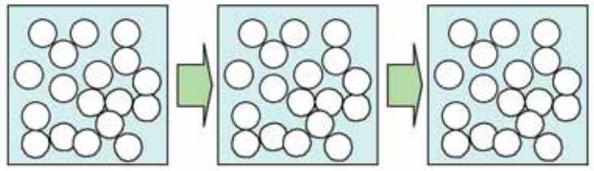

Novel artificial bone: Designed structure can be obtained.

■ ACHIEVEMENTS

(1) Developed novel artificial bone material with both high porosity and strength (10 MPa at 70% porosity: a conventional artificial bone has the same strength at 55%).

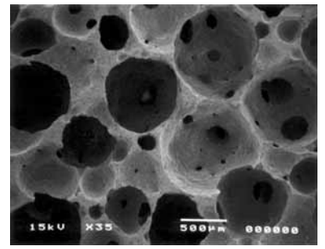

Pore structure of novel artificial bone

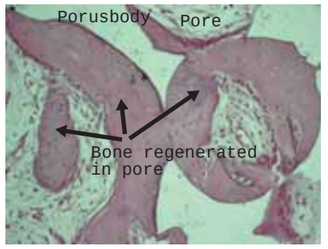

Bone regenerated in pores

(2) Examined the possibility to use as a bone tissue scaffold:Good cell ingrowth and tissue regeneration are observed. (In collaboration with AIST and Osaka University)

(3) Carried out animal tests and pre-clinical tests at Osaka University: Good bone regeneration is observed.

(4) Clinical tests carried out by a private company: The artificial bone is now commercialized, has been applied to over 700 patients and has obtained good clinical results.

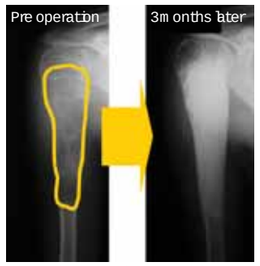

Clinical example: Good bone formation is observed in 3 months.

PUBLISHED RESEARCH PAPERS

1) J. Dong, H. Kojima, T. Uemura , M. Kikuchi, T. Tateishi and J. Tanaka: *J. Biomed. Mater. Res.* 57 (2001) 208.
2) J. Dong, T. Uemura , M. Kikuchi, J. Tanaka and T. Tateishi: *Biomed. Mater. Eng.*. 12 (2002) 203.
3) Japan Patent 3400740, 3470759 and 3718708

ADDITIONAL INFORMATION ABOUT ARTIFICAL BONE

The artificial bone we developed is mainly composed of inorganic hydroxyapatite (HAp: a kind of calcium phosphate) and organic collagen (protein). HAp ceramics were developed separately in Japan and the US in 1975. The direct bone bonding property, called "bioactivity,"was discovered in Japan, and Japanese bioceramics researchers are world-class. However, conventional HAp artificial bones are brittle and have low porosity with low interconnectivity, thus the gold standard for bone defect repair is autologous bone transplantation (autograft: extract self-illium, crash it and implant it in the defect), and artificial bone is only used as an extender if there is insufficient autologous bone. An autograft requires a secondary operation for the normal tissues; therefore, the risks to the patient, such as infection and pain, are quite high. Recently, there has been a high demand for an artificial bone that does not need an autograft. The artificial bone currently used provides sufficient cell and tissue ingrowth ability through improved porosity, interconnectivity and mechanical strength. It can be defined as a second-generation artificial bone that reduces the amount of autologous bone.

Recently, developments in next generation artificial bone materials that do not require an autologous bone transplant have been promoted both in Japan's market (7 billion JPY, potentially 30-35 billion JPY), the US market (65 billion JPY) and the global market. Corresponding with this movement, HAp/collagen nanocomposites with bone-like nanostructures and guided bone regeneration membranes are being studied and developed in the Biomaterials Center, NIMS.

INQUIRIES
Biomaterials Center Masanori Kikuchi, Tetsuya Tateishi
E-mail : KIKUCHI.Masanori@nims.go.jp, TATEISHI.Tetsuya@nims.go.jp

14 Visible Light-sensitive Photocatalyst

■ EXECUTIVE SUMMARY

Photocatalysis - an ideal "green" technology for the decomposition of hazardous chemicals and generation of hydrogen from water using semiconductors and solar light - has long been dreamed of playing a big role in the sustainable development of human life. The ever-expected photocatalyst TiO_2, owing to its large band gap, is practically limited in the existence of ultra-violet (UV) light. In order to utilize the solar energy and indoor illumination more effectively, we have been developing new visible light-responsive photocatalysts with tailored properties via energy band engineering. Some interesting results have been achieved in recent years.

■ OUTLINE

Generally, the typical photocatalysis process over a semiconductor involves the absorption of photons, band gap excitation, separation of the photo-excited electron/hole pairs, and redox reactions on the semiconductor surface (Fig.1). Therefore, the kind of light a semiconductor can absorb depends on its band gap. The well-known TiO_2 photocatalyst has a band gap up to 3.2 eV, which determines that TiO_2 can only respond to UV light. As can be seen from Fig. 2, the UV light only accounts for a small fraction of sunlight, as well as indoor artificial illumination. This seriously limits the application of TiO_2 photocatalysis technology. For a breakthrough, research and development of new photocatalytic materials active under visible light are indispensable.

Up till now, a lot of research has focused on the modification of UV active TiO_2 by doping a different kind of metal (Cr or V) or partial substitution of oxygen ions by other anions, such as nitrogen and sulfur. However, since photo-induced electrons and holes tend to re-combine in the doped level, visible light activation can seldom be expected. Moreover, since the doping amount must be minimal to maintain the crystalline structure of titanium dioxide, the visible light activation effect is limited (up to about 500 nm).

At NIMS, we focused our efforts on the development of novel complex oxides beyond the framework of titanium oxide. Our material design concept is to control the band structures of oxide semiconductors by modulating their electronic structures and crystal structures. The materials are designed to be suitable for the efficient decomposition of organics or splitting of water in a wide range of visible light. The valence state, electronic configuration, effect of crystal field, and the spin and orbital states of constituent were also taken into consideration in our design strategy. On the other hand, to achieve higher efficiency of the developed materials, we applied nanotechnology to increase the surface area and modify the surface structure. Furthermore, the mechanism of the photocatalytic reaction was investigated

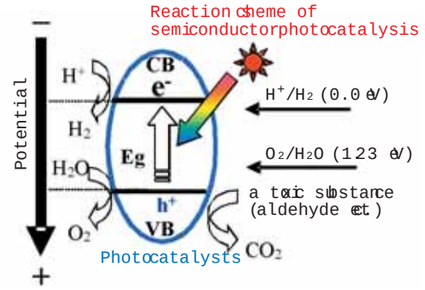

Fig.1 Reaction scheme of semiconductor photocatalysis.

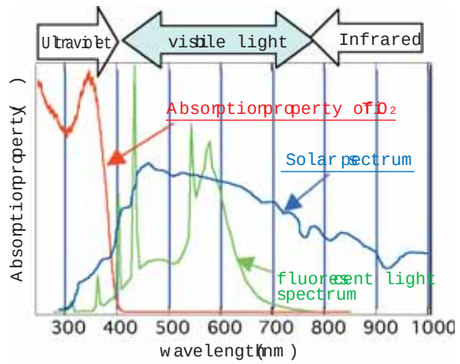

Fig.2 A comparison of absorption property of TiO_2 with spectra of solar and fluorescent lights.

■ ACHIEVEMENTS

(1) We have succeeded in developing the world first photocatalyst Ni-doped $InTaO_4$, which can decompose pure water into H_2 and O_2 gases in the stoichiometric ratio of 2:1 under visible light irradiation (Fig.3, in collaboration with AIST)[1].

(2) Another example of our new photocatalysts is $CaBi_2O_4$, which shows amazingly high activity for photocatalytic decomposition of acetaldehyde, a harmful gaseous organic that causes sick house syndrome (Fig.4). Compared to TiO_2, which is almost inactive under visible light irradiation, the newly developed material showed activity, even if the wavelength of the irradiated light is longer than 540nm. Moreover, the $CaBi_2O_4$ photocatalyst is also effective in the photocatalytic degradation of methylene blue (MB) dye, a dominant contaminant in wastewater[2]. The material is expected as a promising future photocatalyst for indoor and outdoor practical applications.

(3) Photocatalytic water splitting was achieved with a unique type of nanocomposite photocatalyst, Cr-$Ba_2In_2O_5/In_2O_3$, which consists of two individually inactive oxides in nanoscale. The photo-induced charge carrier separation and migration abilities were significantly enhanced due to the ohmic contact formed between different particles. This study suggests a new and important guideline for the development of highly efficient photocatalysts for overall water splitting[3].

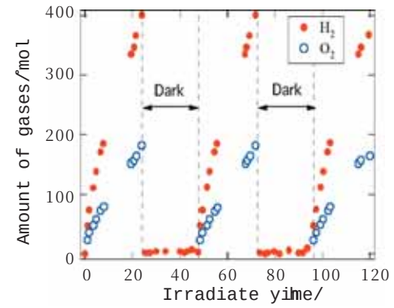

Fig.3 Photocatalytic H_2 and O_2 evolutions on (InNi)TaO_4 photocatalysts from pure water under visible light irradiation.

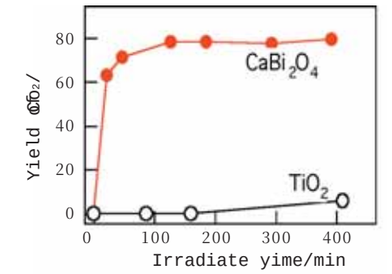

Fig.4 Decomposition ofacetaldehyde over $CaBi_2O_4$ under visible light irradiation.

PUBLISHED RESEARCH PAPERS

1) Zhigang Zou, Jinhua Ye, Kazuhiro Sayama and Hironori Arakawa, *Nature*, 414 (2001) 625.
2) Junwang Tang, Zhigang Zou, Jinhua Ye, *Angew. Chem. Int. Ed.*, 43 (2004) 4463.
3) Defa Wang, Zhigang Zou, Jinhua Ye, *Chem. Mater.*, 17 (2005) 3255.

ADDITIONAL INFORMATION ABOUT PHOTOCATALYST

The TiO_2 photocatalyst is now widely utilized for environmental purification. However, Honda and Fujishima originally documented the TiO_2 for its photo-electrochemical water splitting property. It is interesting that the French writer, Jules Verne, predicted 130 years ago in his famous science fiction novel, "The Mysterious Island", that fossil fuel would one day be exhausted and that H_2 and O_2 from water would supply an inexhaustible source of heat and light. Photocatalytic water splitting is definitely the ideal technology to make this prediction come true. This is dependant on whether a highly efficient visible light-sensitive photocatalytic material can be developed.

INQUIRIES
Photocatalytic Materials Center Jinhua YE
E-mail：Jinhua.YE@nims.go.jp

15 Development and Application of Cold Rolled Ni_3Al Foils

■ EXECUTIVE SUMMARY

Ni_3Al is known as an excellent high-temperature structural material. However, it is very difficult to cold-roll into thin foils due to of its brittleness. We have improved the brittleness using unidirectional solidification and, for the first time, succeeded in fabricating thin foils of Ni_3Al with a 23 mm thickness, which is comparable to that of aluminum and copper. In addition, we found catalytic activity in the Ni_3Al foils and it is now possible to produce hydrogen from methanol and methane using its catalytic activity. Because of their heat resistance and catalytic activity, Ni_3Al foils show potential as the material for fuel reforming microreactors in fuel cells.

■ OUTLINE

"Brittle" is a common feature of intermetallic compounds, and thus very few people make an attempt to fabricate their thin foils by cold rolling. Ni_3Al, which has excellent heat-resistance, is one of the intermetallic compounds that suffer from the same brittleness. This problem was overcome by the addition of a small amount of boron, but the ductility was not high enough to be able to cold-roll into foils as thin as that in aluminum and copper. Alternatively, we developed a method that suppresses a generation of brittle grain boundaries using unidirectional solidification, resulting in substantial ductility improvement. Using this method, we have for the first time succeeded in cold-rolling into thin foils of 23 mm thickness without intermediate annealing, as shown in Fig.1(a). Such heavy cold-rolling is very unusual in intermetallic compounds.

Cold-rolled Ni_3Al foils per se are lacking in ductility. However, moderate ductility emerged after heat treatment in the grain growth stage. As a result, bending and laser welding became possible, which enabled us to fabricate or assemble devices. Fig.1(b), honeycomb structure, shows an example of this.

In this development process, we revealed many fundamental characteristics of Ni_3Al foils, e.g. microstructure and texture of the cold-rolled foils, cold rolling deformation mechanism, evolution of microstructure and texture during heat treatment and mechanical properties of the cold-rolled and heat-treated foils.

Fig.1 (a) A 23 mm-thick cold-rolled Ni_3Al foil and (b) honeycomb structure.

The mechanical properties of Ni_3Al have received much attention due to their excellent high-temperature strength and anomalous temperature dependence of yield stress, and thus there was no idea other than the application for the high-temperature structural materials. Paying special attention to the high concentration of nickel in Ni_3Al, we discovered catalytic activity. Methanol decomposes into H_2 and CO over the Ni_3Al foils at temperatures above 450℃ due to their catalytic activity (Fig.2). Catalytic activity is normally observed on fine particles or porous materials that are catalytically active and of high surface area, and is rarely observed on flat foils. The reason for the high catalytic activity is that fine Ni particles supported on carbon nanofibers are spontaneously formed on the foil surface, as shown in Fig.3. We consider that the fine Ni particles function as a catalytic center, and the carbon nanofibers as an inhibitor of the agglomeration of Ni particles. In addition to methanol decomposition, we found that Ni_3Al foils exhibit a high catalytic activity for methane steam reforming. We fully expect that Ni_3Al foils are the new promising catalyst for hydrogen production.

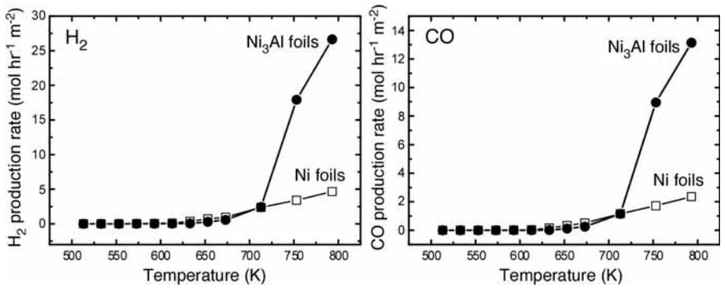

Fig.2 Catalytic activity in cold-rolled Ni_3Al foils for methanol decomposition.

TEM image

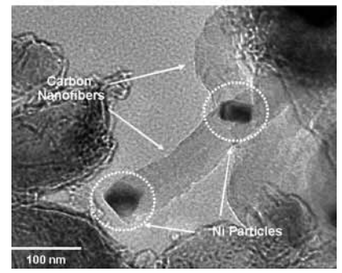

Fig.3 Spontaneous formation of fine Ni particles supported on carbon nanofibers.

The results demonstrate that Ni_3Al foils possess a bi-function for high-temperature structural properties and catalytic activity, the existence of which is very rare. We believe that it is possible to fabricate microreactors for hydrogen production using Ni_3Al foils alone. Needless to say, hydrogen is the important fuel in a fuel cell and a microreactor is a small and highly efficient fuel reforming device.

■ ACHIEVEMENTS

(1) For the first time ever, we succeeded in fabricating cold-rolled Ni_3Al foils of a 23 mm-thickness.
(2) We developed a technique to control the microstructure of cold-rolled Ni_3Al foils through heat treatment, resulting in improvements of the mechanical properties. We also developed a laser welding technique of the foils.
(3) We discovered that cold-rolled Ni_3Al foils exhibit catalytic activity for methanol decomposition.
(4) We revealed that the catalytic activity is ascribed to the spontaneous formation of fine Ni particles supported on carbon nanofibers on the foils during catalytic reactions.

PUBLISHED RESEARCH PAPERS

1) M. Demura, K. Kishida, Y. Suga, M. Takanashi and T. Hirano: *Scripta Mater*. 47(2002)267.
2) K. Kishida, M. Demura, Y. Suga and T. Hirano: *Phil. Mag*. 83(2003)3029.
3) Y. Xu, S. Kameoka, K. Kishida, M. Demura, A.P. Tsai and T. Hirano: *Intermetallics* 13 (2005)151.
4)D.H. Chun, Y. Xu, M. Demura, K. Kishida, M.H. Oh, T. Hirano, and D.M. Wee: *Cat. Lett.*, 106(1-2)(2006)71.

ADDITIONAL INFORMATION ABOUT INTERMETALLIC COMPOUNDS

Intermetallic compounds are a kind of alloy in which two or more constituent metal elements are arranged in order, forming a long-range ordered structure. In Ni_3Al, Ni and Al atoms occupy the face-centered and corner positions of a cubic structure, respectively. This structure contrasts with conventional alloys, such as iron, copper and aluminum alloys, in which constituent metal elements are randomly arranged. Shape memory alloy NiTi, superconducting alloys Nb_3Sn and V_3Ga, and high-temperature structural alloys TiAl and Ni_3Al are used practically.

INQUIRIES
Fuel Cell Materials Center Toshiyuki Hirano
E-mail: HIRANO.Toshiyuki@nims.go.jp

16 Superalloys

■ EXECUTIVE SUMMARY

Advanced gas turbines and aeroengines with higher thermal efficiencies are expected to be the key technologies for mitigation of the global warming due to the energy related CO_2 emissions. To realise these, new alloys for turbine components with higher temperature capabilities are desired. In HTMC, the world leading 5th generation SC superalloys usable up to 1100 degree C were successfully developed in the context of "High Temperature Materials 21 Project Phase 1 (F.Y.1999-2005)" and now followed by the Project Phase 2 (F.Y.2006-2010) targeting a temperature capability as high as 1150 degree C.

■ OUTLINE

With using our alloy design software, we control the lattice misfit between gamma and gamma ' phases in superalloys to be as large as possible. The larger lattice misfit enhances a formation of so-called rafted structure, a sandwich-like structure of gamma and gamma 'phases perpendicular to the stress direction along <100>, and also a denser interfacial dislocation network (Fig.1). Also we add platinum group metals, specifically Ru, to stabilise the microstructure. The created microstructure effectively strengthens the SC superalloy at high temperatures. Coating materials and other high temperature alloys are also being developed.

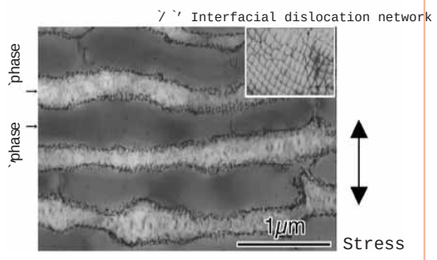

Fig.1 Microstructure in alloy TMS-138.

■ ACHIEVEMENTS

On the basis of the alloy design concept described above, as shown in Fig.2, we successfully developed 4th and 5th generation SC superalloys and reached the Phase 1 target, 1100 degree C, with a 5th generation alloy TMS-196 and some others[1),2)]. A 4th generation alloy TMS-138 was tested successfully in a supersonic engine test bed (Fig.3). These alloys are expected to be used in advanced gas turbines and aeroengines being developed in some private companies.

The latest turbine blades are coated with metallic and ceramic materials and cooled inside by air to survive the hot gas with temperatures beyond 1500 degree C, which is even higher than the melting points of the superalloys. Here the compatibility between coatings and the substrate superalloys is an issue. We developed a new metallic coating, named as EQ (thermo-dynamically equilibrium) coating, which is under evaluation for practical use 31.

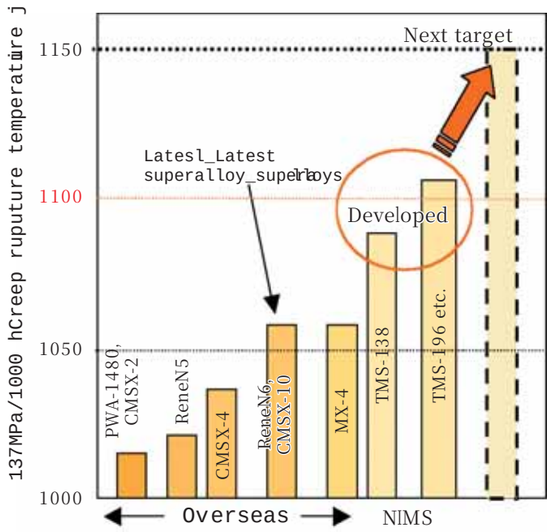

Fig.2 Temperature capabilities of SC superalloys.

As the turbine gas temperature increases, cast & wrought turbine disc materials for use at beyond 700 degree C are also needed. In HTMC we designed Ni-Co base new superalloys for this purpose and 1.7 tons of ingots were produced and successfully forged to near net shape discs. Also, refractory superalloys with gamma and gamma ' phases have been developed based on platinum group metals, specifically Ir[4)]. It has been found that these alloys have a superior oxidation resistance compared with Nb and W base alloys, as well as excellent high temperature strengths. Cr-Re alloys with excellent ductilities were also developed.

Following these results, NIMS and Rolls-Royce PLC, U.K., jointly established The Rolls-Royce Centre of Excellence for Aerospace Materials at NIMS. This Centre aims at developing new generation SC superalloys for the Trent engines powering Boeing 787 and Airbus 350XWB.

Fig.3 A turbine blade made of TMS-138 and the supersonic engine test on the test bed.

PUBLISHED RESEARCH PAPERS

1) J.X.Zhang, T.Murakumo, Y.Koizumi, T.Kobayashi, H.Harada, S.Masaki Jr., *Met.Mat.Trans.A* 33A, 3741-3746, (2002).
2) A.Sato, H.Harada, T.Kobayashi, T.Murakumo, J.X.Zhang, T.Yokokawa, *Journal of Japan Institute of Metals,* 70-2, 196-199(2006).
3) A.Sato, H.Harada, K.Kawagishi, *Met.Mat.Trans.A, Vol.37A,* 789, March (2006).
4) Y.Yamabe-Mitarai, Y.F.Gu and H.Harada, *Platinum Metals Review,* 46, (2), 74-81 (2002).

ADDITIONAL INFORMATION ABOUT SUPER ALLOYS

Ni-base superalloys consist of gamma solid solution based on Ni and gamma' precipitate based on Ni_3Al ordered phase. Because of the two phases being coherent each other, the created interphase interface acts as barrier against the dislocation motion resulting in the higher creep strength of the superalloys. The Ni-base superalloys have evolved from wrought alloys to conventionally cast (CC) alloys, directionally solidified (DS) alloys, and then single crystal (SC) alloys. SC alloys are also evolved from the 1st generation (0%Re), 2nd generation (3%Re), 3rd generation (5-6%Re), and now 4th generation (2-3%Ru) and 5th generation (5-6%Ru) alloys are being developed. The latest SC alloy in practical use is the 3rd generation alloy CMSX-10.

INQUIRIES
High Temperature Materials Center Hiroshi Harada
E-mail : HARADA.Hiroshi@nims.go.jp

17 Development of Superconducting Tapes and Wires –MgB_2 and Nb_3Al–

■ EXECUTIVE SUMMARY

We have developed tapes and wires for MgB_2 and Nb_3Al superconductors that we expect will be used in various technological fields. Improvements in critical current density (J_c) which is the most important property for practical applications, were developed by the control of microstructures. 100m - 1km-long MgB_2 and Nb_3Al tapes and wires were successfully fabricated, and small superconducting coils were fabricated from these tapes and wires. Successful excitations of these coils clearly indicate that MgB_2 and Nb_3Al superconducting tapes and wires are promising for future applications in various technological fields.

■ OUTLINE

The new intermetallic superconductor, MgB_2, which was discovered in Japan in 2001, shows a high transition temperature Tc of about 40K. Tape and wire fabrication of MgB_2 is now being studied worldwide due to its potential application to liquid-helium-free or liquid-hydrogen-cooled devices. Low materials cost is another advantage of MgB_2.

NIMS has started the development of MgB_2 tapes and wires, applying the so-called powder-in-tube method just after the discovery of MgB_2, in order to obtain high performance MgB_2 tapes and wires (Fig.1). We carried out microstructure control and additions of impurities to improve the critical current density (J_c) of the tapes and wires. We found that another important parameter, the upper critical field (B_{c2}) of the tapes and wires, is on the practical level. We also fabricated 100m-long tapes and wires and constructed small coils using these tapes and wires to evaluate the possibility of practical applications of MgB_2 tapes and wires[1)].

Regarding Nb_3Al, the degradation of superconductivity with mechanical strain (or electromagnetic stress) is much less than the commercial Nb_3Sn, which has the same crystal structure as Nb_3Al. Thus the study to fabricate a long-length of Nb_3Al wire for next generation high-field and large-scale superconducting magnets has been carried out over two decades. Difficulties in commercialization lie in the nature of the phase diagram. The stoichiometry is stable only above 1700℃, but the Al composition of Nb_3Al becomes poor below 1000℃, so we developed a rapid heating, quenching and transformation (RHQT) technique to overcome this difficulty. A Nb/Al precursor wire is continuously joule-heated, quenched into molted Ga and the resultant bcc Nb-25at%Al supersaturated-solid solution filaments embedded in the Nb matrix are transformed into the stoichiometric Nb_3Al filaments by additional annealing at 800℃. For practical use, the establishment of the large-billet making technique (Fig.2), a uniform RHQ operation of a wire over 1 km class (Fig.3), and the incorporation of a Cu stabilizer, is ongoing

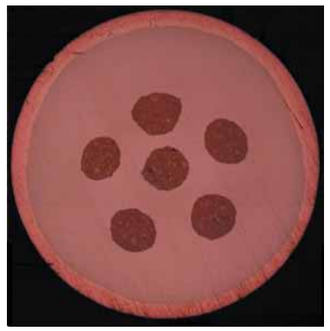

Fig.1 Cross section of MgB_2 multifilamentary wire. @ @(outer diameter: 1.2mm)

Fig.2 Nb-Al large billet.

Fig.3 Continuous rapid heating and quenching apparatus.

■ ACHIEVEMENTS

We enhanced the Jc for MgB_2 tapes and wires by improving MgB_2 grain connectivity and impurity additions, such as SiC and hydrocarbons. B_{c2} at 20K of MgB_2 tapes and wires is around 9-10T, which is comparable to that of commercial Nb-Ti at 4.2K, suggesting that MgB_2 is promising for 20K applications.[2)] Furthermore, we fabricated small MgB_2 solenoid coils and succeeded in generating a magnetic field with a MgB_2 coil for the first time. One of the coils generated a field of 1.3T (1T bias field) at 20K. Field generation above 1T at 20K, together with high B_{c2} at 20K, suggest that we can construct convenient high performance cryo-cooler-cooled or liquid-hydrogen-cooled MgB_2 coils without liquid helium.

Regarding Nb_3Al, we made a 2.6 km piece of multifilamentary precursor wire without any breakages by installing a large-scale RHQ apparatus. We also succeeded in establishing a uniform RHQ technique over 1 km and manufacturing a 1 km class Cu stabilized wire. Superconducting properties of the head and tail of long length of wire are in agreement with each other. To demonstrate the uniformity of long wire, we manufactured a Nb_3Al insert-coil that was assembled in a Nb-Ti/Nb_3Sn outer-coil (406/100 mmΦ) and succeeded in generating an additional 4.5 T in a 15 T bias field. The total magnetic field of 19.5 T is the highest record of a superconducting magnet operated at 4.2 K.

Fig.4 Example of MgB_2 solenoid coil (Outer diameter: 48mm, Inner diameter: 30mm, Height: 50mm. Number of turns: 459).

PUBLISHED RESEARCH PAPERS

1) K. Tanaka, *et al., Fabrication and transport properties of an MgB2 solenoid coil, Supercond. Sci. & Technol.* 18(2005)678-681.

2) H. Kumakura, *et al., Upper critical fields of powder-in-tube-processed MgB_2/Fe tape conductors, Appl. Phys. Lett.* 84(2004)3669.

3) K.Tagawa, *et al., Trial manufacture of a km class length of Cu cladding RHQT Nb_3Al flat-wire, IEEE Trans. Appl. Supercond.* 16(2006)1168.

ADDITIONAL INFORMATION ABOUT SUPERCONDUCTING TAPES AND WIRES

Superconductivity, which realizes a large flow of electric current without any resistivity, is very interesting from a practical application aspect. We now expect superconductivity to be utilized in various areas, such as energy, environment, medicine/biotechnology, transportation, etc. These superconductor technologies can resolve various worldwide problems, including CO_2 emission, indicating that superconductivity is one of the key technologies for welfare in the 21st century. High performance superconducting tapes and wires are essential for the practical application of superconductivity, thus research and development of such high performance tapes and wires are now actively being carried out around the world.

INQUIRIES
Superconducting Materials Center Hiroaki Kumakura
E-mail: KUMAKURA.Hiroaki@nims.go.jp

18 Ultra-fine Grained Steel
–High Strength and High Toughness Steels without Using Alloying Elements–

■ EXECUTIVE SUMMARY

The target to "achieve double strength steel with a double life span, consisting of a recyclable chemical composition without using any rare alloying elements" was introduced according to the basic project concepts of "reducing the environmental load" and "reducing the total cost". A basic technology for a new type of steel-making, consisting of alloy-free steel and impurity permissible steel, was established in our efforts to obtain high strength and durable steels through the refinement of crystal grains.

■ OUTLINE

Achieving double strength steel

One method for solving an environmental issue relating to energy is to reduce the amount of steel use. For example, if the strength of steel were to be doubled, only half of the original amount of steel would be necessary. The most commonly used steel at present is a heavy gage welding steel with a strength of 400 MPa, which is used in bridges and buildings. Although 800 Mpa steel (alloy steel) already exists and is being manufactured, our goal was to create a steel with a strength of 800 MPa that was a completely different type of steel, and did not contain any alloying elements. The drawback of a steel with a small amount of alloying elements is that it is weak, but this problem could be overcome by reducing the grain size of the steel. An increase in the strength from 400 MPa to 800 MPa was obtained successfully by decreasing the grain size from the 10μm to 1μm (Fig. 1).

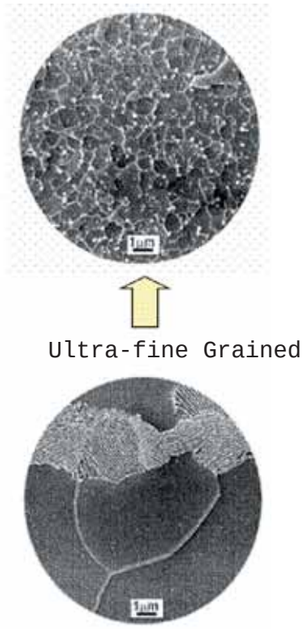

Fig.1 The microstructure of ultra-fine grained steel.

Realization of double strength and double life span

One of the weaknesses of steel is "rusting". At present, Ni and Cu are used in weathering steels, but Ni is expensive and Cu is difficult to recycle. Thus, we proposed a completely new and different type of weathering steel using recyclable low cost Al-Si. The preliminary experiment confirmed that the atmospheric corrosion quality of the new steel was equal to that of the Ni type weathering steel. However, Al and Si are elements that cause steel to become brittle; therefore, they cannot be applied as materials for large earthquake proof structures. The basic research on grain refinement, which has been conducted since 1997 demonstrated its power to resolve this situation. The refinement of grains was shown to improve not only the strength, but also the Charpy impact toughness (ductile-brittle transition temperature). Thus, by using a sample with a composition of 0.1C-1.5Mn-0.8Al-0.8Si (wt%), the tensile strength of the thick plate that was produced at 600℃ doubled when the grain size was refined to 1μm. Other required characteristics, including a room temperature absorption energy of 200J and a ductile-brittle transition temperature of below -100℃ were also satisfied (Fig.2). The target of double strength and double life span could be achieved by this method, without using any rare elements.

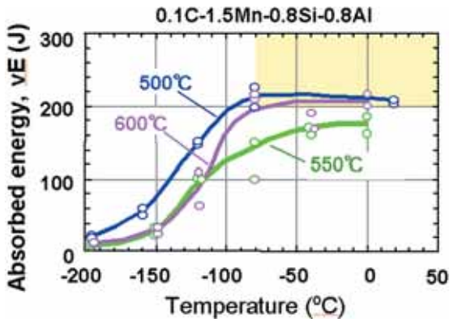

Fig.2 Toughness of ultra-fine grained Al-Si added steel (results of the Charpy test).

■ ACHIEVEMENTS

(1) The details of the processing conditions for the refinement of crystal grains (processing temperature, strain rate, strain amount, stain components, cooling rate after processing) were examined, and the different processing methods were found to be especially effective for grain refinement.
(2) The production of ultra-fine grained high strength steels in various forms, such as rods and thick plates (35mm), was shown to be feasible by applying the principle for grain refinement, which was established in the laboratory, to equipment actually used in production (Fig.3)
(3) By applying the grain refining technology to Al-Si steel, a new high strength and durable weathering steel with outstanding recyclability was proposed, and the project target of double strength × double life span (factor 4) was achieved.
(4) A highly efficient low heat input welding technology, such as ultra-narrow gap arc welding and defect-free deep penetration laser welding, which does not damage the base metal characteristics of ultra-fine grained steels, was developed.

Fig.3 Various forms of ultra-fine grained steel.

PUBLISHED RESEARCH PAPERS

1) T. Inoue, J. Cho, F. Yin, K. Nagai: *Journal of the Japan Institute of Metals,* 69 (2005), 341-347.
2) S. Torizuka: *Bulletin of the Iron and Steel Institute of Japan,* 10 (2005), 185-195.
3) Patent Registration Numbers 3543104, 3525180
4) Domestic Patent 2005-105325
5) K. Hiraoka, S. Tsukamoto: *Journal of the Japan Welding Society,* 74 (2005), 102-108.

ADDITIONAL INFORMATION ABOUT RECYCLABLE HIGH STRENGTH STEEL

To begin with, pure steels are not very strong - if anything, they are soft and fragile. The general way to strengthen steel is to make it into a compound, in other words to form an alloy. For example, the strength of steel can be increased by adding carbon, Cr, Mo, etc. The thick plate welding steels with a strength of 800 MPa that are currently being manufactured utilize alloys. However, steels that contain alloying elements are difficult to weld, expensive, and require lots of energy for recycling. High strength steels (alloy free steels: ultra-fine grained steels) that do not require alloying are a new generation of structural material that overcomes the problems relating to resources, environment, and energy.

Our research found that it is even possible to use alloying elements that are brittle, since the toughness can be improved to an epoch-making degree by refining the grain size to 1 ˚m. In other words, the refining technology of grains widens the selection of alloying elements and provides us with the possibility of a new steel manufacturing technology. The total weight of all the materials that are produced in Japan is approximately 2 hundred million tons per year. Steels are ranked first and account for approximately one hundred million tons of that total. Therefore, recycling steel is important for the continuance of society. The above mentioned "grain refinement", which produces "recyclable alloy free steel" and "impurity permissible steel" can be described as a 21st century materials technology that supports a recycling society.

INQUIRIES
Structural Metals Center Kaneaki Tsuzaki,
URL: http://www.nims.go.jp/stx-21/
E-mail: TSUZAKI.Kaneaki@nims.go.jp

19 High Nitrogen Stainless Steel –Resource Saving High Corrosion-resistant Steels–

■ EXECUTIVE SUMMARY

Using the two technologies of the addition of nitrogen and the purification of material, resource saving corrosion-resistant steel applicable to marine and offshore environments has been developed. To fabricate this new material, a pressurized Electro-Slag Remelting (P-ESR) furnace was newly developed in Japan by NIMS. High corrosion-resistant nitrogen steel was successfully developed using this furnace.

■ OUTLINE

Fabrication of HNS using the P-ESR method:

Fig.1 shows the principle of the pressurized ESR method. Flux heated by an electric current was converted to a molten status, which melted the primary electrode. In this process, high-purified material was obtained by the refining effect of the slag. FeCrN powder was used as the nitrogen source. Flux used in the research was a combination of CaF_2、CaO、and Al_2O_3, all of which were added to the crucible prior to each test. The phase diagram of 23%Cr-2%Mo series steel calculated by Thermocalc is shown in Fig.2. As shown in the figure, it was found that the material was single austenitic phase, the Ni content was reduced with increasing nitrogen content and, finally, that Ni-free HNS was obtained when the nitrogen content was higher than 1.2 mass %.

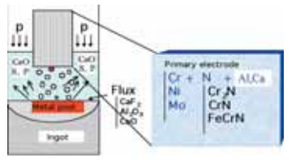

Fig.1 Principle of pressurized ESR method.

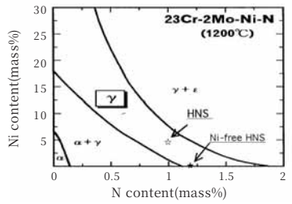

Fig.2 Phase diagram of HNS.

Mechanical properties:

Fig.3 shows the mechanical properties of 23 mass% Cr series HNS after solution treatment in terms of elongation and strength of HNS, together with relevant data for comparison.
From this figure, it was found that the strength of γ single phase HNS is about 1.5 times higher than that of SUS304, while the elongation of HNS is almost equivalent to that of SUS304. In addition, it was also found from data tested separately that HNS maintained high strength properties in a wide temperature range of up to 500℃, and their yield ratio (proof stress/tensile stress) varied from 0.5 through 0.6. The elongation and reduction of area of HNS was almost equivalent to that of SUS316.

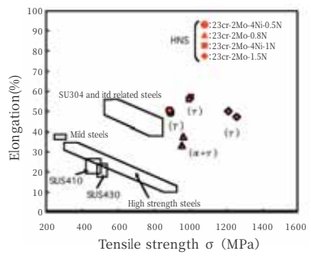

Fig.3 Mechanical properties of HNS.

Corrosion properties:

HNS crevice corrosion tests were carried out using multi-crevice assembly in artificial seawater at 35℃. Two types of HNS were used: one was 23%Cr-4%Ni -2%Mo-1%N by the P-ESR method, and the other 16.5%Cr-14%Ni-4%Mo-0.2-0.5%N by the solution nitriding method. Fig. 4 shows the crevice corrosion test results in terms of crevice corrosion potential (CCP) and nitrogen content.

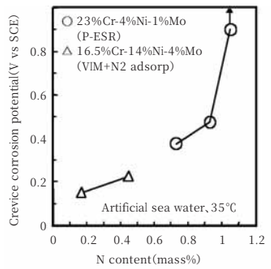

Fig.4 Crevice corrosion property of HNS.

From these results, it was found that crevice corrosion was observed on the surface of the solution nitrided specimens up to 0.5%N, while the HNS specimens by P-ESR showed no crevice corrosion, even at high potential of oxygen evolution. In addition, HNS specimens, tested by the P-ESR method, were tested in actual seawater and no crevice corrosion has been observed more than 2.5 years later.

■ ACHIEVEMENTS

(1) High nitrogen bearing steel, of which the nitrogen content is more the 1 mass%, was successfully fabricated by the pressurized ESR method. In addition, as shown in Fig. 5, various products of HNS were trial manufactured, showing the potential for practical use in the near future.
(2) To improve corrosion properties, nitrogen was added and it was found that dissolved nitrogen ion reacted with hydrogen ion, yielded from the hydrolysis reaction of metals, and resulted in the production of ammonium ion. Thus, lowering the local pH was suppressed.
(3) Ni-free austenitic HNS was successfully developed due to the high nitrogen content. This material is promising as an anti-Ni-allergy material in the bio/medical field. Fig. 6 shows an example of a mouthpiece for wind instruments, made by Ni-free HNS in a collaborative work between the "STX21 Collaborative Research Group" in Suwa district, Nagano-prefecture and NIMS.

Fig.5 Samples of various products of HNS.

Fig.6 Mouthpiece made from Ni-free HNS.

PUBLISHED RESEARCH PAPERS

1) Y. Katada, M. Sagara, Y. Kobayashi and T. Kodama, *Materials and Manufacturing Processes*, 19, 1 (2004) 19-22.
2) Y. Katada and M. Sagara, Rust Prevention & Control, Japan, 48, 9 (2004), 329-334.
3) M. Sagara et al.: *ISIJ International*, 43, 5 (2003), 714-719.

ADDITIONAL INFORMATION ABOUT CORROSION-FREE STEELS

The economic loss of metallic materials in Japan due to corrosion is up to a few % of the GNP, the predominant materials of which are steels. It is very important to develop corrosion-free steels from the viewpoint of its impact on our social infrastructure, especially as Japan surrounded by water.

Although stainless steels are well known as typical examples of corrosion-free steels, which are fabricated by the addition of anti-corrosion elements, such as Cr, Ni, Mo, the use of stainless steels is quite limited. In fact, stainless steels cannot be used in seawater, where the integrity of passivation films cannot be maintained for long periods due to chlorine ions.
The target of this research is to develop a new anti-corrosion nitrogen-bearing steel, without the addition of too much Cr, Ni, Mo.

INQUIRIES
Materials Manufacturing and Engineering Station Yasuyuki Katada
E-mail：KATADA.Yasuyuki@nims.go.jp

20 Synthesis and Structure analysis of Quasicrystals

■ EXECUTIVE SUMMARY

More than 20 years have passed since the discovery of quasicrystals in 1984. The majority of quasicrystals were discovered by NIMS during these years. Quasicrystals have a peculiar structure and there are some very important quasicrystals in existence that show they are highly efficient as the methanol dissolving catalysts for obtaining hydrogen fuel. Expecting to produce new quasicrystals with new physical properties, for the last five years we have tried to synthesize new stable quasicrystals by replacing Cd atoms in Cd-Yb, Cd-Ca, which were found in 2000, with In and Ag. Many stable quasicrystals have been found so far. However, quasicrystals have no period, so their detailed structures have only been clarified recently. NIMS has developed the structure analysis of crystals without periodicity for more than 10 years. In 2002, we clarified, for the first time, a detailed structure of an icosahedral Al-Pd-Mn quasicrystal and their surface structures were revealed in 2004. Furthermore, in 2005, we released a computer software package for the structure analysis of quasicrystals for public use.

■ OUTLINE

We first found Cd-Yb, Cd-Ca and other stable binary quasicrystals in 2000, and it challenged the consensus among scientists that quasicrystals necessitate ternary alloys. After this discovery, several tens of stable quasicrystals were found and they formed the largest group of crystalline approximants and quasicrystals. From 2001-2003, stable quasicrystals in In-Ag-Yb and In-Ag-Ca systems were developed by replacing Cd with monovalent Ag and trivalent In, which are on either side of Cd in the periodic table.[1] This suggests that the Hume-Rothery rule, which states that a specific structure is stabilized by a specific valence electron density, is efficient. By applying this rule, stable quasicrystals, including tetravalent elements, such as Zr and Hf, were also found.

In addition to these quasicrystals, we succeeded in the syntheses of their crystalline approximants, which are conventional crystals with periods, but their local atom arrangement is similar to those of quasicrystals. Therefore, they are important for understanding quasicrystal structures. We made phase diagrams of the In-Ag-Yb and In-Ag-Ca systems and we confirmed that their 1/1 and 2/1 crystalline approximants had a chemical composition similar to the corresponding quasicrystals. In addition we succeeded in growing a single domain quasicrystal of 1cm³. We could not find stable quasicrystals in the Zn-Mg-Ti and Zn-Mg-Eu systems, but we achieved 1/1 and 2/1 crystalline approximants. Among them, the structure analysis of 1/1 approximants of Zn-Mg-Hf was performed, and it was clarified that they are composed of two kinds of chemically different atom clusters. From this fact, we can infer that F-type Zn-Mg-Hf icosahedral quasicrystals are composed of two similar kinds of clusters.

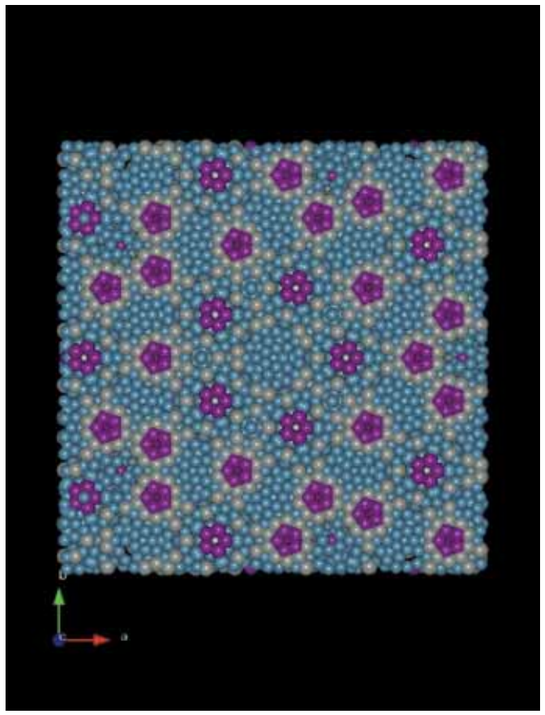

Fig.1 A surface structure normal to a five-fold axis in Al-Pd-Mn quasicrystals.

In the icosahedral quasicrystals, there is no period in any direction and, as a result, their detailed structures have not been clarified, even after more than 15 years since they were first discovered. Therefore, the understanding of their physical properties and surface structures remains difficult. In the present study, we succeeded for the first time in the structure analysis of icosahedral quasicrystals in the Al-Pd-Mn system by applying a method that describes a non-periodic structure as a periodic structure in a higher-dimensional space.[2] We studied this method for a long time. We know that icosahedral quasicrystals are given from a periodic structure in a 6 dimensional space by taking a 3 dimensional intersection, so once we know the 6 dimensional structure, we can immediately obtain all the atom positions in a 3 dimensional space. There are several methods by which to obtain detailed information about the structures in a 6 dimensional space, but we need to develop computer software so there are no examples of what has been analyzed so far. NIMS proposed a modeling method called the higher-dimensional cluster method, and based on that method we developed a theory of structure analysis and necessary software. According to the results, we clarified the structure of Al-Pd-Mn. In addition, based on this structure, we also clarified the surface structure of Al-Cu-Fe[3], which has a similar structure to that of Al-Pd-Mn. We also released the program package of quasicrystal analysis for general use. Figure 1 shows a surface structure normal to a 5-fold axis in Al-Pd-Mn quasicrystals.

■ ACHIEVEMENTS

(1) Syntheses of In-Ag-Yb, In-Ag-Ca, Zn-Mg-Hf and Zn-Mg-Zr quasicrystals and their crystalline approximants.
(2) The structure analysis of Al-Pd-Mn quasicrystals and the determination of the Al-Cu-Fe surface structure.
(3) The release of a program package for quasicrystal analyses.

PUBLISHED RESEARCH PAPERS

1) J. Hasegawa, S. Takeuchi, A.P. Tsai, *Philo. Mag. Lett.*, 85 (2005) 289
2) A. Yamamoto, H. Takakura, and A. P. Tsai: *J. Alloys Comp.* 342 (2002) 159.
3) H. R. Sharma, V. Fournee, M. Shimoda, A. R. Ross, T. A. Lograsso, A. P. Tsai, and A. Yamamoto: *Phys. Rev. Lett.* 93 (2004) 165502

ADDITIONAL INFORMATION ABOUT QUASICRYSTALS

There is no periodicity in so-called quasicrystals, modulated structures, and composite crystals. The atom arrangement in such crystals can be determined by obtaining a three-dimensional intersection of a 6 dimensional periodic structure. NIMS developed the necessary computer software for their structure analyses and it is available on the Web.

INQUIRIES
Quantum Beam Center Akiji Yamamoto
E-mail：YAMAMOTO.Akiji@nims.go.jp

21 Discovery of A Giant Electrostrain Effect Based on a New Principle

■ EXECUTIVE SUMMARY

NIMS researchers discovered a giant electrostrain effect (i.e., electric-field induced strain) based on a new principle. The strain, induced by an electric field, is about 40 times larger than the conventional piezoelectric effect. Furthermore, unlike the conventional PZT piezoelectric materials, the material showing this effect does not contain hazardous Pb. The new principle is quite general and may be applicable to various materials; it may also provide the possibility to develop novel electrostrictive materials with a large electrostrain effect, while being environmentally friendly.

■ OUTLINE

Electrostrain materials have been widely used as sensors and actuators due to their ability to convert between electrical energy and mechanical energy. These applications can be found in mobile phone speakers, the ink-control of ink-jet printers, the ultra-accurate control of the cantilever, at the sample stage in modern scanning tunneling microscopes, etc.

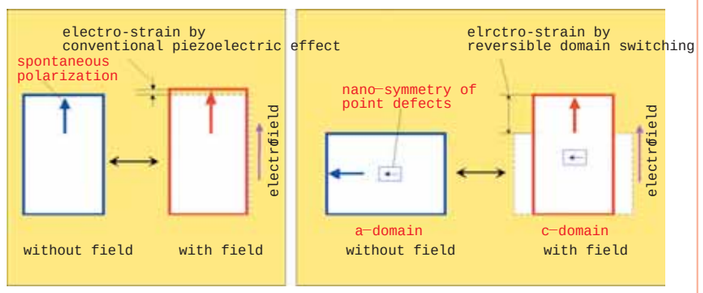

Fig.1 (a) Conventional electrostrain. (b) Giant electrostrain.

The conventional electrostrain effect, i.e., the converse piezoelectric effect, is due to the tiny ionic displacement induced by an electric field (Fig.1a). In principle, such a mechanism can generate only a very small strain, and as a result, even the best material based on this principle, i.e., PZT, can generate a strain of only 0.01% with an electric field of 100V/mm Furthermore, the PZT, which comprises 90% of the world's production of piezoelectric materials, is facing a serious decrease in use, because it contains hazardous Pb and may cause environmental problems. Therefore, developing environmentally friendly, high-performance electrostrain materials is an urgent priority.

On the other hand, electrostrain materials contain ferroelectric domains (Fig.2), which are the different electric polarization areas. Under an electric field these domains move in the same direction as the field direction, and at the same time generate a huge strain due to the exchange of the unequal crystalline axis of the low symmetry ferroelectric phase (Fig.1b). However, such domain switching is usually irreversible and thus this effect has been of no practical use. NIMS researchers utilized a general symmetry property of point defects (imperfections in the crystal) and succeeded in creating a reversible domain switching. As a result, they achieved the giant electrostrain effect (Fig.3).

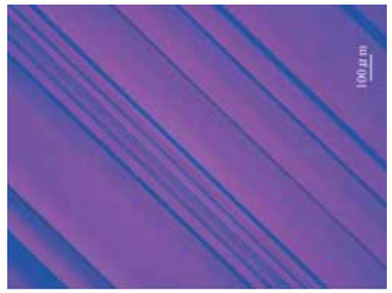

Fig.2 Domains in ferroelectrics.

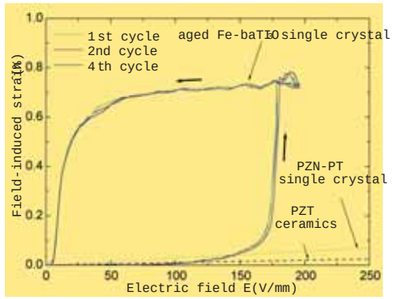

Fig.3 Giant electrostrain effect based on the new principle.

■ ACHIEVEMENTS

The electrostrain effect of Fe-doped $BaTiO_3$ single crystal is shown in Fig. 3. At a low field of 200V/mm, a huge strain of about 0.75% is achieved. This value is about 40 times larger than that of the typical PZT if compared at the same field, and about 10 times larger than that of the high-strain PZN-PT single crystals. Furthermore, we found that a large electrostrain effect also exists in K-doped $BaTiO_3$ single crystals; this suggests that the new mechanism is a general one[1]. It is expected that the giant electrostrain effect may open new areas of applications due to its large effect. Another important feature of the new discovery is that the materials showing such a remarkable effect do not contain hazardous Pb, making them possible candidates for environmentally friendly high-performance electrostrain materials.

NIMS researchers recently made one further step; they applied the new principle to polycrystalline ceramics and found a large non-linear electrostrain effect[2]. This is an important step in applying this effect in an industrialsetting. Very recently, evidence for the new electrostrain principle has been found,[3,4] which solidifies the physical basis of this new principle. The in-situ optical microscopy experiment has confirmed the existence of reversible domain switching.

PUBLISHED RESEARCH PAPERS

1) X. Ren, *Nature Materials*, 3, (2004) 91-94
2) L.X. Zhang, W. Chen and X. Ren, *Appl. Phys. Lett.*, 85, (2004) 5658-5660
3) L.X. Zhang and X. Ren, *Phys. Rev. B*, 71, (2005) 174108—16
4) L.X. Zhang and X. Ren, *Phys. Rev. B*, 73, (2006) 094121—6.

ADDITIONAL INFORMATION ABOUT ELECTROSTRAIN EFFECT

The electrostrain effect is the conversion of electrical energy into mechanical energy, although its converse effect, the piezoelectric effect, is more widely known. Generally, materials showing an electrostrain effect or piezoelectric effect are called piezoelectric materials, but they should be referred to as "electrostrain materials" if they are used to generate strain/force by electricity.

INQUIRIES
Sensor Materials center Xiaobing Ren
URL: http://www.nims.go.jp/ferroic/
E-mail: Ren.Xiaobing@nims.go.jp

1 Formation of a High-Field NMR Complex

■ EXECUTIVE SUMMARY

The 920 MHz and 930 MHz NMR magnets were developed using two kinds of Nb_3Sn superconductors developed by NIMS. Both magnets broke the world record at that time. Six NMR spectrometers have been used for research of structural biology, solid-state NMR, etc. at Sakura site.

■ OUTLINE

An NMR spectrometer is an indispensable tool for organic chemistry and is installed in many laboratories across many industries. The sensitivity and resolution of an NMR spectrometer are improved with an external magnetic field. A high-field NMR spectrometer is in high demand by bioscience researchers to determine the 3D structure and functions of protein molecules. It also enables the measurement of quadrupole nuclei, such as ^{27}Al and ^{17}O, the NMR signals of which are difficult to detect with a middle-field NMR spectrometer.

The magnetic field of an NMR spectrometer is generated by a superconducting magnet. NIMS had a number of epoch-making achievements in high-field superconducting magnets by applying their newly developed superconductors. Two kinds of newly developed Nb_3Sn conductors were applied to the 920 MHz and the 930 MHz NMR magnets. An increase in the high fields critical current was achieved by increasing the tin content in the bronze matrix. A 15 wt% tin content Nb_3Sn conductor (formerly 13 wt%) was applied to the 920 MHz magnet, while a 16 wt% conductor was used for the 930 MHz magnet. A high-strength Nb_3Sn conductor reinforced with tantalum was employed for the both magnets, as shown in Fig. 1.

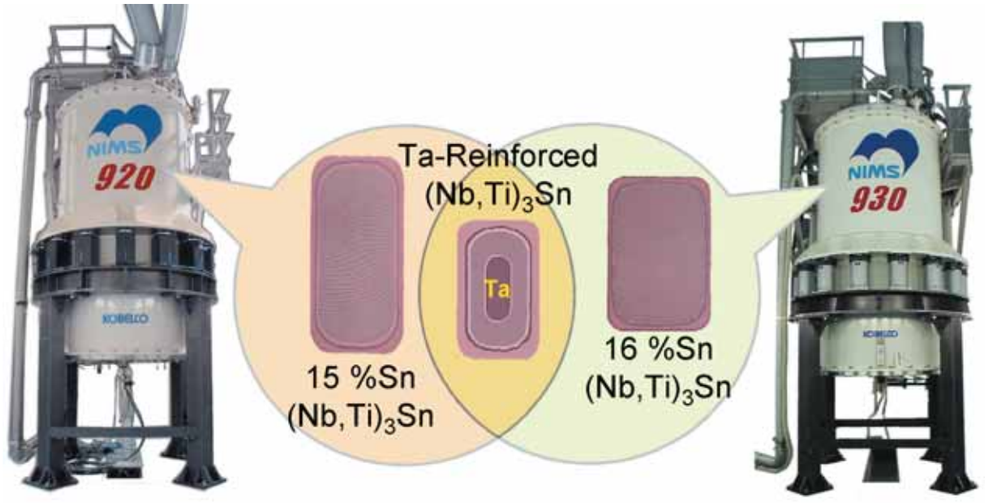

Fig.1 The 920 MHz and 930 MHz NMR magnets. The newly developed Nb_3Sn conductors are also shown.

■ ACHIEVEMENTS

At Sakura site, six NMR spectrometers, including the four systems shown in Fig.2, have been used as user facilities and they form a high-field NMR complex. The 920 MHz NMR spectrometer is used for solution NMR measurements. In a collaborative study with the Genomic Sciences Center, RIKEN, the 3D structure of protein molecules was determined, as shown in Fig.3[1]. The 930 MHz NMR spectrometer is used in the new research field, "high-field solid-state NMR" and NMR probes to measure quadrupole nuclei have also been developed. Many kinds of materials, such as inorganic catalysts, semiconductors and steel making slag, have been measured with the spectrometer.[2]

A 920 MHz NMR spectrometer is now commercially available. The second spectrometer has operated at the Institute for Molecular Science as a cooperative shared facility.

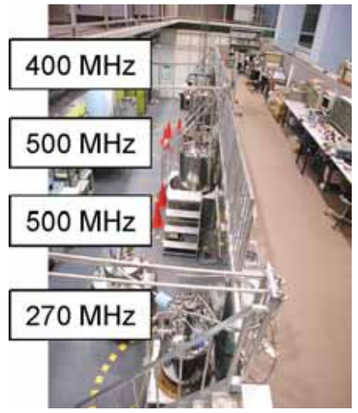

Fig.2 NMR spectrometers for solid-state NMR.

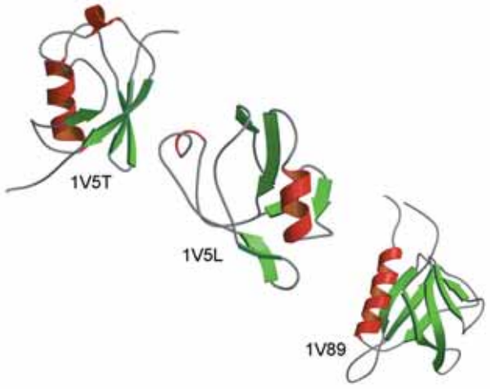

Fig.3 3D structures of protein molecules determined with the 920 MHz NMR spectrometer. The Protein Data Bank ID numbers are indicated.

PUBLISHED RESEARCH PAPERS

1) T. Kiyoshi, H. Maeda, J. Kikuchi, *et al., IEEE Trans. Appl. Superconduct.* 14 (2004) 1608-1612.

2) T. Iijima S. Kato, R. Ikeda, *et al., Chemistry Letters* 34 (2005) 1286-1287.

ADDITIONAL INFORMATION ABOUT NMR

The letters NMR stand for nuclear magnetic resonance. It uses a resonance phenomenon that, in some kinds of nuclei, occurs at a certain radio frequency proportional to the magnetic field. NMR is a non-destructive method and amorphous, surface, boundary, or projection parts in materials can be analyzed. Chemical and geometrical information can also be obtained. Four Nobel Prizes were given for NMR research. MRI (magnetic resonance imaging) used for medical diagnosis is based upon the same phenomenon.

As the proton has the highest sensitivity in the practical nuclei, it has been the main nucleus in the NMR measurements. The resonance frequency is absolutely proportional to the magnetic field. In the case of a proton, the resonance frequency of 1000 MHz corresponds to 23.48 T. The performance of an NMR spectrometer is drastically improved with a magnetic field, and they were historically named according to the proton resonance frequency of their magnetic fields, such as a 920 MHz NMR spectrometer. An NMR magnet generates an extremely stable magnetic field, which does not vibrate with a MHz frequency.

INQUIRIES
High Magnetic Field Station Tsukasa Kiyoshi
E-mail : KIYOSHI.Tsukasa@nims.go.jp

2 The Internet Electron Microscopy System

■ EXECTIVE SUMMARY

We have developed a remote-control electron microscopy system and have been using it for research projects and scientific outreach programs. We aim to promote efficient and effective collaboration without the time and cost expended by researchers' travel time, as well as specific science education through the use of actual microscopes.

■ OUTLINE

In this research project, we have developed a remote-control electron microscopy system that people can use to access and observe images from anywhere in the world via the Internet. The system allows collaboration between researchers and engineers, remote analysis, and characterization. It is also suitable for scientific outreach programs so that students or the general public can experience the nano-world for themselves. We are running the system at a collaborator ' s institute for collaboration and at a national museum and several high schools for outreach.

Unlike optical microscopes whose magnification ranges from several hundreds to several thousands, electron microscopes typically have high magnification ranging from several tens of thousands to several millions. Due to their high performance, electron microscopes are essential instruments for state of the art science and technology. They are also highly effective for scientific education and outreach, so students and the general public can experience real and practical science and technology for themselves. However, not everyone can access electron microscopes due to their high cost, and the expertise required for maintenance and sample preparation.

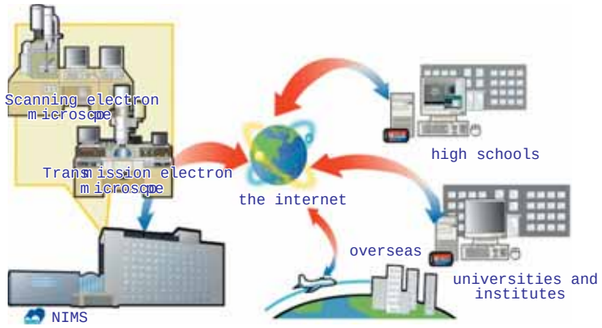

Fig.1 The Internet Electron Microscopy system.

The electron microscope we developed is located at the National Institute for Materials Science, and is carefully adjusted and maintained. Our engineers carry out sample preparations and installation. Remote clients, who are located at the science museum and various high schools, can independently access the microscopes and perform remote-operations using their web browsers on the Internet. The utilization of current broadband networks allows us to promote innovative outreach programs for discovery learning.

The system is quite useful for research collaboration. The researchers used to travel back and forth to use microscopes at other institutes, which consumed a lot of time and money. With this system, each researcher can stay at his/her own laboratory, and still conduct experiments with other members and discuss the results at the same time.

Our system stores data and user information securely, as well as web-based scheduling of microscopes. Multi access and operation by the collaborators are also possible. We aim to develop a model system applicable to all kinds of remote-controllable experimental instruments.

■ ACHIEVEMENTS

The client terminal has been in operation for four years at the National Museum of Emerging Science and Innovation in Tokyo. More than one thousand visitors have used the system, more than two-thirds of which were students from elementary and high schools. Most of them appreciated the new and impressive experience of the nano-world they observed.

The client terminals are installed at several super science high schools designated by the Ministry of Education, Culture, Sports, Science and Technology. The terminals are frequently used in Science classes and in science clubs. The students plan their research topics and conduct individual experiments. They collect or make samples, send them to NIMS, whose engineers then prepare them as microscope specimens and insert into the microscopes, and observe the specimens during their allocated observation time. Their research results have been presented at scientific contests and junior sessions of national scientific meetings. Demonstrations are also frequently carried out at various events.

A terminal installed at an institute of technology is being utilized as one of the project tools for the fabrication and observation of nano-structures.

PUBLISHED RESEARCH PAPERS

1) K. Furuya *et al., Microsc. Microanal.* 11, S2, 68-69 (2005)
2) A. Tameike *et al., Microsc. Microanal.* 10, S2, 1566-1567 (2004)

ADDITIONAL INFORMATION ABOUT ELECTRON MICROSCOPES

Electron microscopes magnify sample images by illuminating them with electron beams. While optical microscopes use light as their illumination source, the use of electron beams, the wavelength of which is much smaller than light, produce a significantly high resolution. Typical maximum magnification of optical microscopes is about several thousand, but using an electron microscope, it is quite common to observe samples using magnification greater than a million. It is also possible to analyze the elements of the samples using x-rays generated by electron beam illumination.

There are two types of electron microscopes: scanning electron microscopes (SEMs) and transmission electron microscopes (TEMs). SEMs use the electron beams generated from the surface of the sample when electron beams are illuminated on them, and form three-dimensional images. TEMs transmit electron beams through very thin samples and by observing their structures, it allows high resolution observation at a magnification of more than one million. In the Internet Electron Microscopy project, we use SEMs for outreach and a TEM for collaboration.

INQUIRIES
High Voltage Electron Microscopy Station Kazuo Furuya
URL : http://www.nims.go.jp/it_em/ENG/
Email: it_em@nims.go.jp

3 Creation of a Structural Materials Datasheet

■ EXECUTIVE SUMMARY

To construct a secure and safe society, it is necessary to enhance the reliability of various structural materials that comprise transport facilities, including railroads and automobiles, as well as mechanical structures, such as power plants and chemical plants. To use materials safely and effectively, we create material data specifying properties such as creep, fatigue, and corrosion, and make it available to the public as structural materials datasheets.

■ OUTLINE

We conduct long-term creep tests on heat resistant metals to be used in hostile environments of high temperature and pressure to obtain long-term creep test data that covers more than 100,000 hours (approximately 11 years and 5 months) as shown in Fig. 1, and issue the data in creep data sheets. We provide standard data to ensure the safe use of materials, as well as examine creep strength evaluation methods, mainly targeting the 22 types of new heat resistant metals that were developed after 1980, although when we started this project in 1966, there were 44 types of heat resistant metals to test.

Fig. 2 shows a fatigue fractured surface with internal destruction from an inclusion within the material. Since the strength of the material becomes higher and the life of the mechanical structure becomes longer, the degradation of strength from fatigue due to internal destruction has become an issue at the level of 10 billion cycles, which is a higher cycle than ever before. To address this, we examined the possibility of applying an ultrasonic fatigue test, and established an accelerated testing technology that can evaluate the fatigue strength properties of a gigacycle within one week, although the conventional testing method for the cycle would require more than three years. We issue data obtained from these tests as fatigue data sheets, which helps improve the safety and reliability of mechanical structures.

Expenditure for preventing metallic materials from corrosion corresponds to about 1% of the GDP (Source: Japan Society of Corrosion Engineering, 2001), so it is clear that we need to develop weathering steel that will be effective in reducing expenditure for corrosion prevention. Consequently, we have been conducting long-term exposure tests on Fe-X binary alloys and obtaining basic atmospheric corrosion data, together with weather observation data to issue corrosion data sheets.

An analysis of the H-II Rocket No.8 accident in November 1999, revealed that the strength evaluation of materials used for the liquid hydrogen rocket engine was insufficient. In fact, the fatigue strength of titanium alloy at extremely low temperatures (4K) varies greatly depending on the shape of the product, as shown in Fig. 3. To enhance the reliability of materials used for domestically-designed rockets, we have been obtaining material property data relating to tension, Charpy impact, fatigue, fracture toughness, etc., of materials used for fuel turbo pumps and engines of H-IIA rockets and the next-generation of reusable rockets, to issue the data as the Space Use Materials Strength Data Sheet.

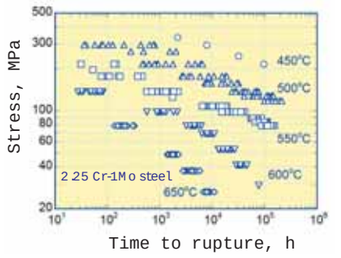

Fig. 1 Stress-creep rupture time data of 2.25 Cr-1Mo steel.

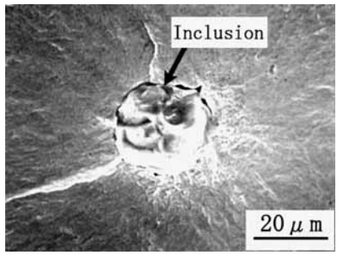

Fig. 2 Fatigue fractured surface with internal destruction from an inclusion within the material.

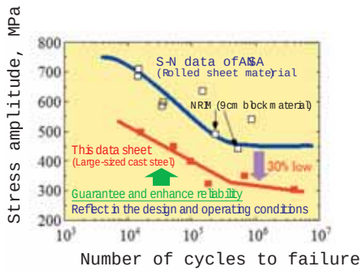

Fig. 3 Fatigue strength property of Ti-5Al-2.5Sn ELI alloy at 4K.

■ ACHIEVEMENTS

We have been studying creep and fatigue for more than 30 years, and will have issued 130 volumes of creep data sheets, five volumes of metallographic atlas of crept materials, and 102 volumes of fatigue data sheets by the end of FY2005. Regarding corrosion and space use materialsstrength, we have been studying this field since FY2001, and have issued three volumes of corrosion data sheets, one volume of corrosion atlas, and 10 volumes of space use materials strength data sheets. These results have been available to the public not only as printed materials, but also via the Internet, as a part of the NIMS Materials Database[1].

Regarding high Cr ferritic heat resistant steel, the need to reevaluate long-term creep strength and review allowable stress based on the reevaluation has been pointed out both domestically and internationally, due to reports of damage caused by degradation of long-term creep strength, such as pipe fracture. The region splitting analysis method"[2] of creep strength proposed by NIMS, where 50% of 0.2% offset yield stress is set as a boundary condition, was used to review the allowable tensile stress stipulated in the Interpretation of the Engineering Standard for Thermal Power Plants"[3] and to the formula for evaluating the remaining life of existing plants, thus contributing to the improvement of safety and reliability of high-temperature plants. These results have also been referenced by standard development organizations in Europe and the U.S.

The results of space use materials strength data sheets have been used in the design evaluation and verification of operating conditions for first and second stage engines of H-IIA rockets since the first successful launch in August 2001, contributing to greater reliability of subsequent rocket engines.

PUBLISHED RESEARCH PAPERS

1) NIMS Materials Database: http://mits.nims.go.jp/

2) Kazuhiro Kimura, Hideaki Kushima, Fujio Abe. *J. Soc. Mat. Sci.,* 52 (2003) 57

3) *Interpretation of the Engineering Standard for Thermal Power Plants,* Nuclear and Industrial Safety Agency, Ministry of Economy, Trade and Industry. NISA-234c-05-8, December 14, 2005

ADDITIONAL INFORMATION ABOUT CREEP

High-pressure containers, such as gas cylinders, must be safe and must never break or burst. For this reason, allowable stresses for materials used for such containers are prescribed, and containers are designed and manufactured within the allowable stress values. A material deforms elastically if it is pulled with little force, and returns to its former size if the force is removed. When it is pulled with a force greater than the elastic deformation limit, plastic deformation occurs, meaning it does not return to its former shape, which may eventually lead to rupture. The maximum force until rupture corresponds to its tensile strength, and the strength of the material. Since one-quarter of the tensile strength is set for allowable stress, sufficient safety is secured. Nevertheless, if the material is exposed to a high temperature, even a small elastic deformation may cause continuous deformation over time, which is sufficient to lead to eventual rupture. This phenomenon, which depends on the passage of time, is called "creep", and creep rupture becomes an issue at high temperatures exceeding approximately one-third of the melting point (absolute temperature) (approximately 400 degrees C and over for steels). Therefore, allowable stress at high temperatures is determined by the stress to cause rupture at the end of 100,000 hours (approximately 11 years and 5 months). To ensure safety for materials used in the high-temperature environments of thermal power stations, chemical plants, etc., it is important to conduct proper material evaluations for long-term creep strength.

INQUIRIES

Materials Data Sheet Station Kazuhiro Kimura
URL: http://www.nims.go.jp/mdss/english/E_index.htm
E-mail address: KIMURA.Kazuhiro@nims.go.jp

4 The Success of the Development of Wavelength-dispersive FE-EPMA for Submicron Region Analysis

■ EXECUTIVE SUMMARY

The electron probe micro analyzer (EPMA) with a wavelength-dispersive X-ray spectrometer (WDS) mounted on the field emission (FE) type electron gun was successfully developed for the first time (Fig.1). In traditional-EPMA models, the analysis performance was the only area that was over several microns. However, the smallest size that can be analyzed with this newly developed equipment is 1/10 or less, which is less than 100nm. In addition, it also shortened to 1/4 or less in the time taken for the two-dimensional plane analysis. This new equipment greatly contributes to the research and development of advanced materials.

■ OUTLINE

The ultra-high vacuum over 10^{-8} Pa is needed to use the stable FE electron gun. However, due to a large sample chamber and X-ray spectrometer with a complicated transfer mechanism (a maximum of 5 spectrometers are mounted), the vacuum degree of a traditional EPMA model is about 10^{-4} Pa. A differential ion pump will generally compensate for this four-digit difference in pressure. However, the ion pump action can become unstable due to a slight PR gas (Ar + CH_4) leak from the X-ray detector. The electron probe from the FE electron gun was not stabilized, so the middle room (installed between the electron gun and sample chamber) was placed in the electron optics vacuum system, as shown in Fig.2, then the exhaust system of the electron gun was separated from the exhaust system of the sample chamber (the X-ray spectrometer was connected with the sample chamber), and both exhausted independently. As a result, the sufficient exhaust speed required to stabilize the operation of the FE electron gun was ensured to obtain more positive ultra-high vacuum conditions. In addition, by adopting the Schottky type in the FE electron gun, the current value and stability of the electron gun necessary for the EPMA was obtained.

Fig.1 Overview of the new FE-EPMA (Prototype).

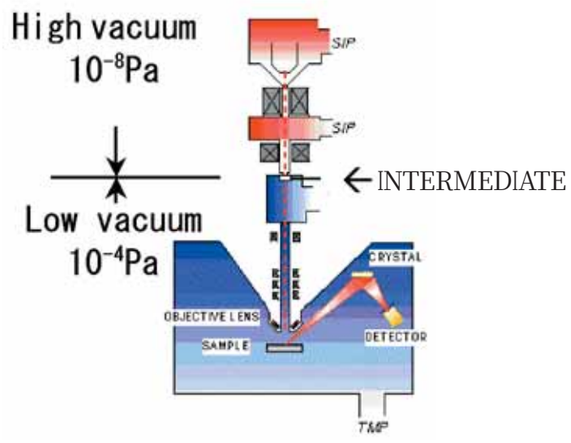

Fig.2 Schematic diagram of the evacuation system of the new FE-EPMA.

■ ACHIEVEMENTS

In Fig.3, the relationship between the size of the analysis region and the beam current required to analyze the boundary of Ni and Cu, is shown. It is proven that this new equipment can analyze smaller regions, which can be analyzed with the traditional EPMA model using W filaments, across all ranges. Fig.4 is the result of observing the distribution of the Ni-Si compound. The minute distribution of the chemical compound shown by the arrow marks is clearly observed.

The new EPMA model, which was completed by this study, has already been commercialized, and over of 30 new-model EPMAs are placed domestically and overseas. The new-model EPMA covers a wide range of fields, such as metals, minerals, ceramics, plastics, fibers, biological specimens, etc. and it is utilized for structure evaluation and failure analysis in those fields.

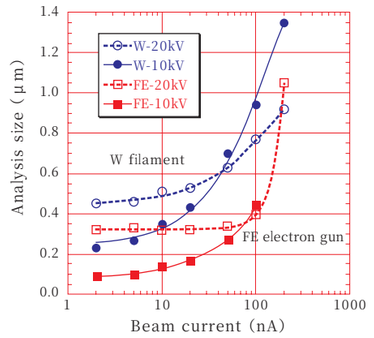

Fig.3 Relationship between beam current and analysis size using Ni/Cu junction.

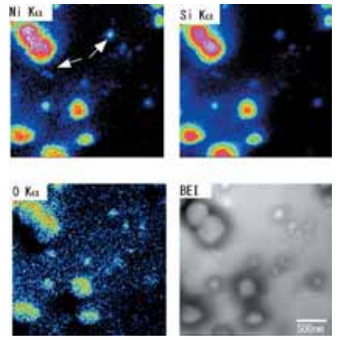

Fig.4 Example of high-speed mapping Ni-Si submicron particles in highly pure copper. 10keV-30nA 40ms/pixel (approximately 107min).

PUBLISHED RESEARCH PAPERS

1) Takashi KIMURA, Kenji NISHIDA, and Shigeo TANUMA : *Journal of Surface Analysis,* 10,3(2003)203-211
2) Takashi KIMURA, Kenji NISHIDA and Shigeo TANUMA : *Microchimica Acta,* 155 (2006) 175-178

ADDITIONAL INFORMATION ABOUT EPMA

EPMA measures X-rays and reflection electrons, secondary electrons and cathode luminescence, which rise from irradiation from the electron beam focused under several °m meter in the sample. This equipment is utilized in many fields as a powerful analysis technique that measures observation of material structures, component element concentration of micro areas, present state of chemical compounds, etc.

By mounting the FE electron gun in EPMA, the spatial resolution, which seems to have already reached the limit, was also improved by over 10 times. This new equipment has made it possible to accurately and quickly analyze the material structure of sub-micron regions, which was previously thought to be impossible, and advanced materials research is expected to develop further.

INQUIRIES
Materials Analysis Station Shigeo Tanuma, Takashi Kimura
E-mail: TANUMA.Shigeo@nims.go.jp, KIMURA.Takashi@nims.go.jp

THE OTHER ACCOMPLISHMENTS

- Development of first-principles simulation techniques to analyze transport properties of next-generation nano-materials such as organic molecules and DNA
- Experimental study on the liquid-liquid critical point hypothesis of water
- Development of self-formation technique of quantum dots by droplet epitaxy
- Semiconductor quantum dot for quantum cryptography communication
- Development of terahertz band high frequency devices using intrinsic Josephson effect in high-Tc superconductors
- Preparation of TiO_2 nanotubes on a glass substrate
- Cadmium Hydroxide Nanostrand
- Fullerene nanowire
- Plasma-synthesized TiO_2 nanoparticles with a unique non-equilibrium defect structure generated through ordering of high-concentration oxygen vacancies
- Development of electrochromic hybrid polymers
- Development of high-quality refractory zirconium boride single crystals
- Assembly of photonic crystals in SEM
- Advanced Electronic Material exploration by combinatorial methodology
- Material development for innovative nano-DDS
- Diamond superconductors
- Novel technique for formation of TiO_2 thin film on a PET resin
- Development of nitrogen-doped porous titania powderes with visible-light photocatalytic activity
- Development of solid electrolytes and electrode materials for fuel cells
- Warm Spray–A new coating process using warmed powder particles at high velocity–
- Development of fine metallic powder production by hybrid atomization process

Materials Research Infrastructure

- Promotion of international standardization of testing methods and evaluation methods for materials by the VAMAS activities
- Development of Ultra-Soft X-ray Spectrometer(100eV or less) for Electron Probe Microanalysis
- Electron beam induced fabrication of nano-magnet and the characterization of its property by electron holography technique
- The development of high resolution and low temperature Lorentz electron microscope and the analysis of domain structures of nano magnetic materials
- The analysis of low temperature and crystal structures of materials with strongly-correlated electrons by using high resolution electron microscopy
- SQUID microscope

Management of the First Mid-Term (Data Collection)

Transition of Research Achievements

Transition of the number of papers and patent applications

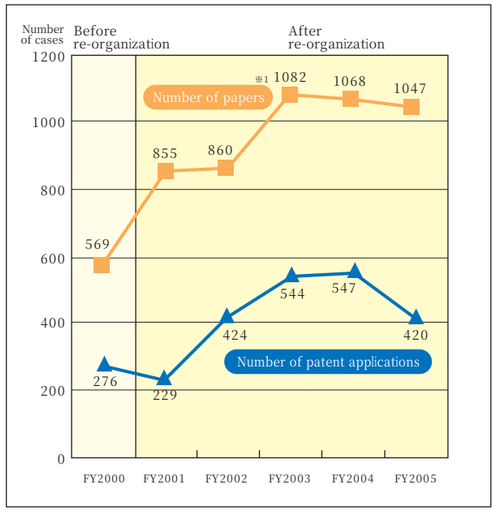

※1 The numbers of papers are recorded by calendar year.

Ranking of the number of quoted papers (Materials Science) ※2

Before re-organization (1996～2000)		After re-organization (2001～2005)	
1	Max Planck Society (Germany)	1	Chinese Academy of Sciences
2	Tohoku University	2	Max Planck Society (Germany)
3	University of California, Santa Barbara	3	Tohoku University
4	MIT	4	National Institute of Advanced Industrial Science and Technology
5	Russian Academy of Sciences	5	National Institute for Materials Science
6	Cambridge University	6	MIT
7	National Institute of Advanced Industrial Science and Technology	7	CSIC (Spain)
8	Pennsylvania State University	8	The University of Tokyo
9	Kyoto University	9	Cambridge University
10	Osaka University	10	Osaka University
⋮			
31	National Institute for Materials Science※3		

※2 Calculations based on the ESI Database of Thomson Scientific Company in March 2006

※3 Calculations based on the total of the National Research Institute for Metals and the National Institute for Research in Inorganic Materials

Transition of the Number of Papers and IF Values

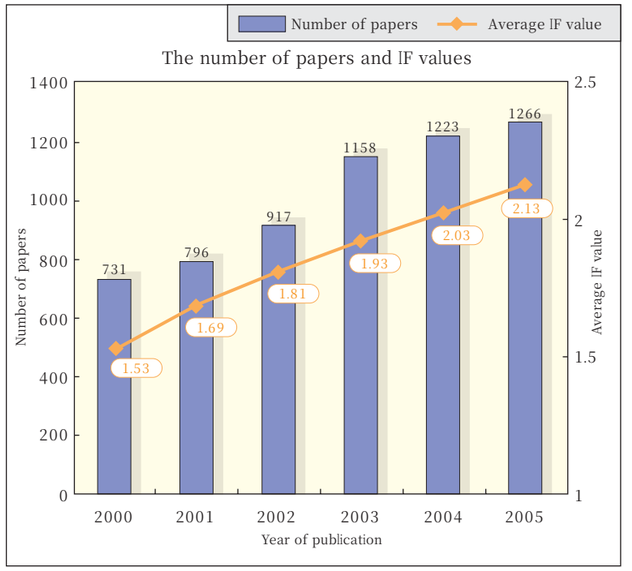

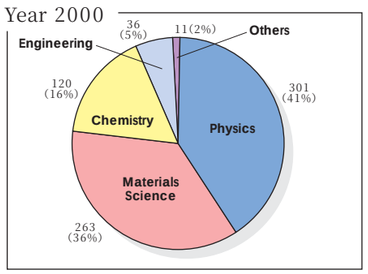

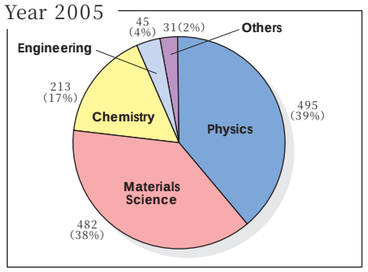

※ Calculations based on the Web of Science database of Thomson Scientific Company

Observations and Findings of Independent Administrative Institutions' Technology-related Activities by the Council for Science and Technology Policy

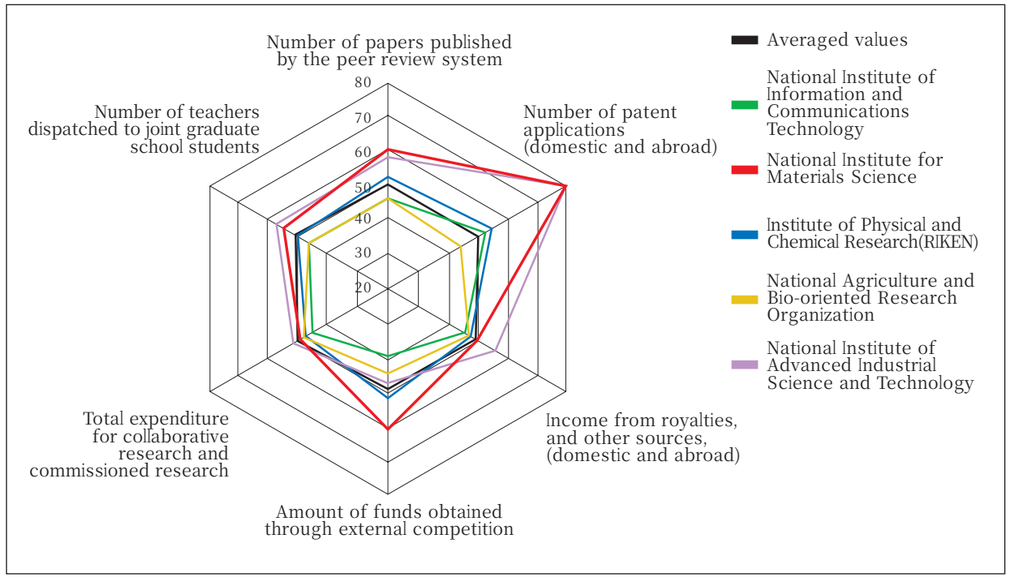

Transition of Operation Subsidies

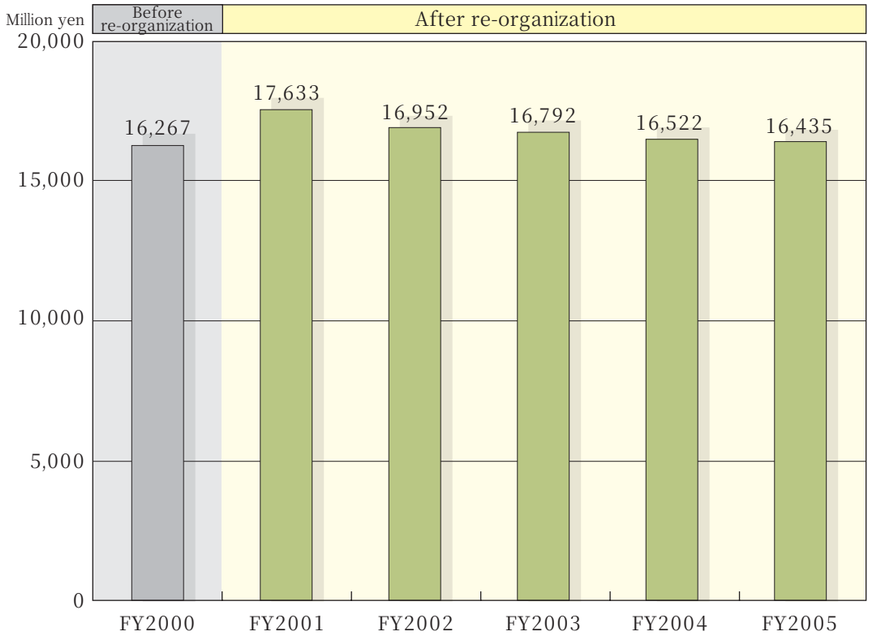

(Notes) In FY2000, budgets were totaled from the former National Research Institute for Metals, and the former National Institute for Research in Inorganic Materials from the general account presided by the Prime Minister's Office. After FY2001, operation subsidies and facilities maintenance expenses subsidies were totaled.

Acquisition Status of External Funds

Research with open-type competitive funds

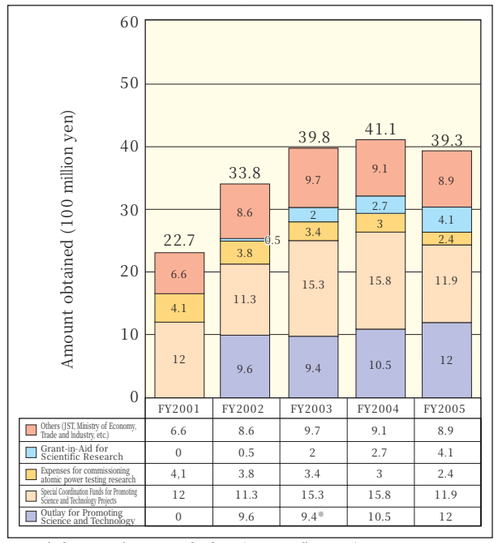

	FY2001	FY2002	FY2003	FY2004	FY2005
Others (JST, Ministry of Economy, Trade and Industry, etc.)	6.6	8.6	9.7	9.1	8.9
Grant-in-Aid for Scientific Research	0	0.5	2	2.7	4.1
Expenses for commissioning atomic power testing research	4,1	3.8	3.4	3	2.4
Special Coordination Funds for Promoting Science and Technology Projects	12	11.3	15.3	15.8	11.9
Outlay for Promoting Science and Technology	0	9.6	9.4※	10.5	12

※ Excluding supplementary budget (1,010 million yen)

Funds from corporations and others

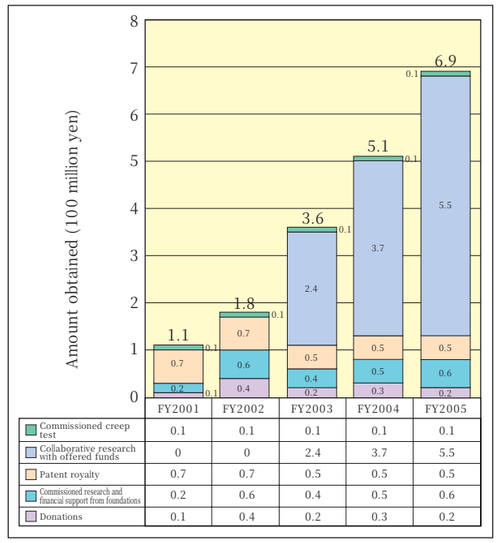

	FY2001	FY2002	FY2003	FY2004	FY2005
Commissioned creep test	0.1	0.1	0.1	0.1	0.1
Collaborative research with offered funds	0	0	2.4	3.7	5.5
Patent royalty	0.7	0.7	0.5	0.5	0.5
Commissioned research and financial support from foundations	0.2	0.6	0.4	0.5	0.6
Donations	0.1	0.4	0.2	0.3	0.2

Acquisition Status of Grant-in-Aid for Scientific Research

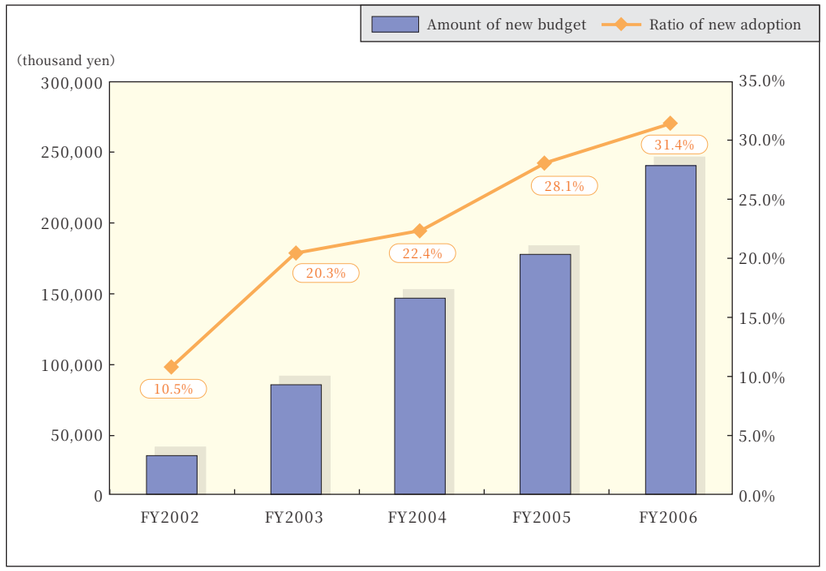

Transition of Achieved Cooperative Activities with Companies

Transition in the number of collaborative research partnerships with companies

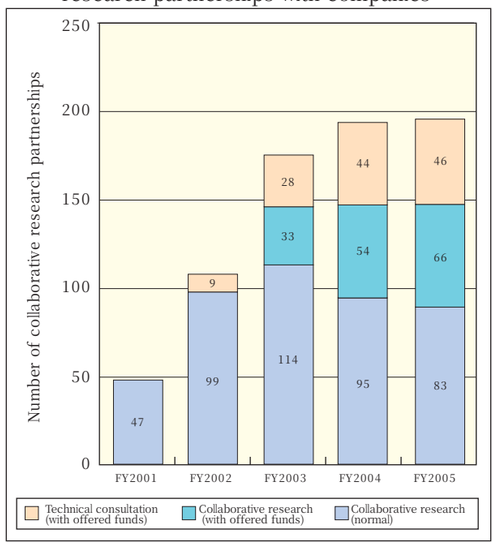

Transition in the number of negotiations for cooperation with companies

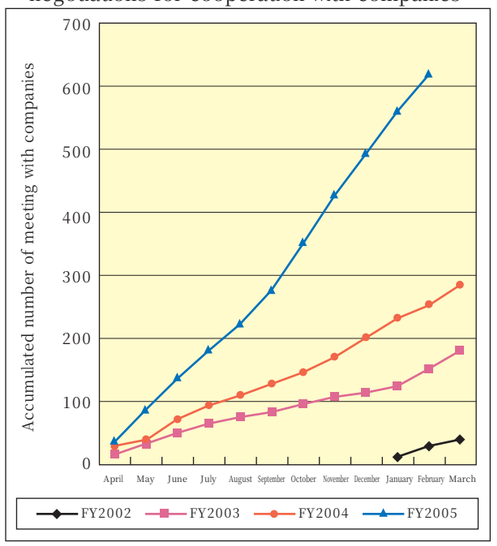

Generation of Venture Companies

Oxide Corporation
(Eestablished October 18, 2000)

- The president assumed the post, putting his research career on hold (The first national institute for testing and research)
- The president retired as of September 30, 2003, to devote himself to company activities
- The company manufactures and sells optoelectronics materials, and others

Awarded the 14th Medium and Small Companies New Excellent Technology/Production Awards, and the Small and Medium Enterprises Prize (April 10, 2002)

NIMS Wave Inc.
(Established May 26, 2004)

- A venture company established in partnership between industry, academy, and independent administrative institutions, namely, between NIMS, Tokyo Denpa Co. Ltd., and Tohoku University
- The company develops high-quality, high-valued added zinc oxide single crystal substrate used for visual devices, including liquid-crystal and plasma displays, as well as manufacturing and sales devices related to zinc oxide

SWING Corporation
(Eestablished May 20, 2003)

- Established in application conjunction with the "NIMS venture company support program" The first venture company of NIMS
- The company manufactures and sells single crystals for holograms, devices for wavelength tuning, etc.

Promotion of venture companies originated from NIMS
NIMS venture company support program

Materials Design Technology Co., Ltd.
(Established September 12, 2003)

- Japan's first venture company established in partnership between industry, academy, and independent administrative institutions, namely, between NIMS, the National Institute of Advanced Industrial Science and Technology, Tohoku University, Kyushu Institute of Technology, and InterScience Ltd.
- The company develops, sells, maintains, and offers consultation and design assistance software services relating to material thermodynamics DB and materials science

Adbic Inc.
(Established September 13, 2004)

- A venture company established by NIMS using the JST Pre-venture project.
- The company develops, designs, manufactures, and sells biotips used to inspect γ-GTP, GOT, and OGPT, which are indicators of hepatic function, using the colorimetry method
- The company also develops and manufactures biotip peripheral devices, such as painless needles

Materials Research Platform

A place to circulate information

Researchers from industry, academy, and independent government organization fields gather to seek a matching point for a break through between seeds and needs

A place for collaborative research

Under the coordination of our institute, plural companies comprise a collaborative research body to promote R&Ds specifying the goal.

※Launched and started operation in FY2005: Ultra-steel, superconductor, opto-single crystal, Pb-free piezoelectric material, super heat-resistant material

Transition of the Number of Full-time Staff

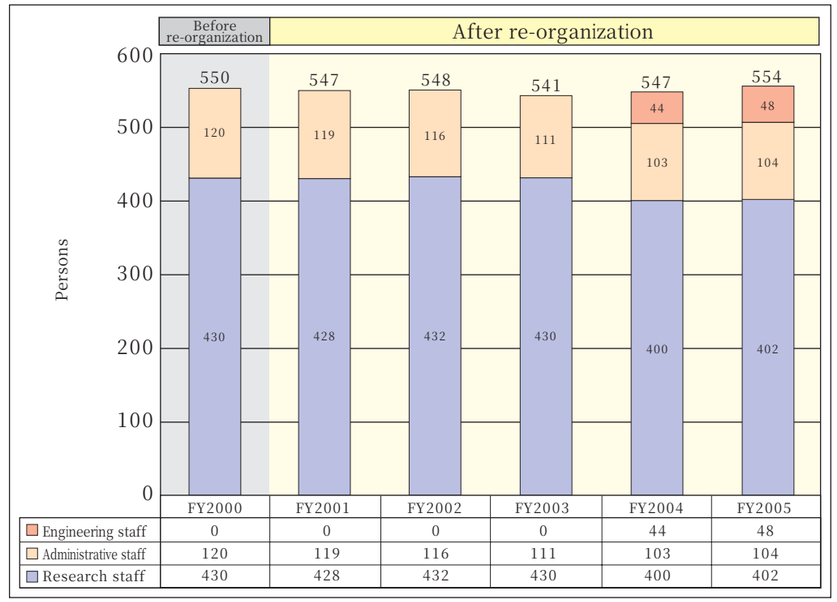

	FY2000	FY2001	FY2002	FY2003	FY2004	FY2005
Engineering staff	0	0	0	0	44	48
Administrative staff	120	119	116	111	103	104
Research staff	430	428	432	430	400	402

Breakdown of Total Staff

Staff category		Number of staff	(Number of females included)	(Number of foreigners included)
Permanent staff	Research staff	402	(21)	(21)
	Engineering staff	48	(3)	(0)
	Administrative staff	104	(16)	(0)
		554	(40)	(21)
Terminable staff		622	(229)	(157)
Visiting Researcher		531	(33)	(63)
Total		1707	(302)	(241)

Issuer: National Institute for Materials Science
(Please contact below for comments and inquiries about this document)

Contact: Kei Kurosawa, Planning and Research Office
1-2-1, Sengen, Tsukuba, Ibaraki, 305-0047, JAPAN
Tel: +81-29-859-2042
Fax: +81-29-859-2025
E-mail : KUROSAWA.Kei@nims.go.jp